REAL-TIME SNOW COVER MAPPING OVER MOUNTAINOUS AREAS OF EUROPE USING MSG-SEVIRI IMAGERY

A THESIS SUBMITTED TO
THE GRADUATE SCHOOL OF NATURAL AND APPLIED SCIENCES
OF
MIDDLE EAST TECHNICAL UNIVERSITY

BY

SERDAR SÜRER

IN PARTIAL FULFILLMENT OF THE REQUIREMENTS
FOR
THE DEGREE OF MASTER OF SCIENCE
IN
GEODETIC AND GEOGRAPHIC INFORMATION TECHNOLOGIES

SEPTEMBER 2008

Approval of the thesis:

REAL-TIME SNOW COVER MAPPING OVER MOUNTAINOUS AREAS OF EUROPE USING MSG-SEVIRI IMAGERY

submitted by **SERDAR SÜRER** in partial fullfillment of the requirements for the degree of **Master of Science in Geodetic and Geographic Information Technologies Department, Middle East Technical University** by,

Prof. Dr. Canan Özgen _____
Dean, Graduate School of **Natural and Applied Sciences**

Assoc. Prof. Dr. Şebnem Düzgün _____
Head of Department, **Geodetic and Geographic Information Technologies**

Prof. Dr. Ali Ünal Şorman _____
Supervisor, **Civil Engineering Department, METU**

Assoc. Prof. Dr. Sevda Zuhal Akyürek _____
Co-supervisor, **Civil Engineering Department, METU**

Examining Committee Members:

Prof. Dr. Vedat Toprak _____
Geological Engineering Department, METU

Prof. Dr. Ali Ünal Şorman _____
Civil Engineering Department, METU

Assoc. Prof. Dr. Mahmut Onur Karslıoğlu _____
Civil Engineering Department, METU

MSc Orhan Gökdemir _____
Beray Engineering

MSc Özgür Beşer _____
Proland Ltd.

Date: _____

I hereby declare that all information in this document has been obtained and presented in accordance with academic rules and ethical conduct. I also declare that, as required by these rules and conduct, I have fully cited and referenced all material and results that are not original to this work.

Name, Last name : Serdar Sürer

Signature :

ABSTRACT

REAL-TIME SNOW COVER MAPPING OVER MOUNTAINOUS AREAS OF EUROPE USING MSG-SEVIRI IMAGERY

Sürer, Serdar

M.S., Department of Geodetic and Geographic Information Technologies

Supervisor : Prof. Dr. Ali Ünal Şorman

Co-Supervisor : Assoc. Prof. Dr. Sevda Zuhal Akyürek

September 2008, 73 pages

An algorithm has been developed for snow recognition (SR) over mountainous areas of Europe from satellite imagery. The algorithm uses Meteosat Second Generations (MSG) instrument Spinning Enhanced Visible and Infra-Red Imager (SEVIRI) data that are acquired in every 15 minutes through whole day. Although SEVIRI has low spatial resolution, its high temporal resolution provides a better discrimination capacity between ice clouds and snow. Discrimination of snow and clouds is the most challenging part of snow recognition algorithm development. The proposed algorithm relies on Satellite Application Facility to support Nowcasting and Very Short Range Forecastings (SAFNWC) cloud products. A final thematic map has

been produced which is consisting of 3 different classes: snow, cloud and land. Validation of the SEVIRI SR product was held in three stages.The obtained high performance of the SR product is presented with the analysis results.

Keywords: Snow, Remote Sensing, MSG-SEVIRI

ÖZ

MSG-SEVIRI GÖRÜNTÜSÜ KULLANARAK AVRUPA ÜZERİNDEKİ DAĞLIK ALANLARDA GERÇEK ZAMANLI KAR HARİTALARI ÜRETİMİ

Sürer, Serdar

Yüksek Lisans, Jeodezi ve Coğrafi Bilgi Teknolojileri Bölümü

Tez Yöneticisi : Prof. Dr. Ali Ünal Şorman

Ortak Tez Yöneticisi : Doç. Dr. Sevda Zuhal Akyürek

Eylül 2008, 73 sayfa

Bu çalışmada uydu görüntüleri kullanılarak dağlık alanlardaki karla kaplı alanların tespit edilebilmesi için bir algoritma geliştirilmiştir. Algoritma meteorolojik bir uydu olan Meteosat Second Generation (MSG) üzerindeki Spinning Enhanced Visible and Infra-Red Imager (SEVIRI) cihazına ait tüm gün içinde alınmış 15 dakikalık görüntüleri kullanmaktadır. SEVIRI'nin yüksek mekansal ve zamansal çözünürlüğü bulut ve kar arasında daha iyi ayırım yapılabilmesini sağlamıştır. Kar ve bulut pikselleri arasında ayırım yapılması geliştirilen algoritmanın en zor kısımlarından biridir. Algoritmada Satellite Application Facility to support Nowcasting and Very Short Range Forecasting (SAFNWC) çalışmasının bulut ürünlerini kullanılmıştır.

Sonuç olarak 3 farklı sınıfın (kar, bulut, kara) ayırımından oluşan bir karla kaplı alan ürünü üretilmiştir. Aynı algoritma ayrıca National Oceanic and Atmospheric Administration Advanced Very High Resolution Radiometer (NOAA AVHRR) görüntüleri üzerinde de uygulanmış ve karla kaplı alan ürünü üretilmiştir. Elde edilen yüksek performans analiz sonuçları ile birlikte sunulmuştur.

Anahtar Kelimeler: Kar, Uzaktan Algılama, MSG-SEVIRI

ACKNOWLEDGEMENTS

I owe the biggest thanks to my family for giving me their endless love and being my family at all, this one is for you.

I would like to express my sincere appreciation to my supervisors Assoc. Prof. Dr. Sevda Zuhal Akyürek and Prof. Dr. Ali Ünal Şorman. From the beginning till the end they have supported me on every situation like a family of my own. I am very grateful to them for giving me the chance to be a part of the H-SAF team, this is and will be the best team that I was involved for the rest of my life for sure.

I am also quite thankful to Orhan Gökdemir and Özgür Beşer for being a real brother and family, sharing their priceless experiences and knowledge with me, I owe you a lot.

Thanks to my examining committee for their valuable suggestions.

I would like to thank Aydın Gürol Ertürk for his highly cooperative approach throughout my MSc study providing me with endless data.

I also would like to thank Aynur Şensoy Şorman and A. Arda Şorman for their valuable supports and motivation.

I want to thank to my beloved friends Onur Kerimoğlu and Burçak İçli for encouraging me to use LaTeX.

I am thankful to Murat Gökdemir for soothing chats during the hard times and Ender Taşdelen for being a great flat-mate .

The GGIT Lab staff: Serkan, Ali Özgün, Musa, Mustafa Kemal, Onur, Aslı, Gülcan, Dilek, Kıvanç, Reşat, and Pınar deserves a credit for their supports.

Dedicated to Galileo Galilei

TABLE OF CONTENTS

LIST OF TABLES

LIST OF FIGURES

CHAPTER 1

INTRODUCTION

Monitoring of the snow covered area (SCA) is a challenging work for the meteorologists and climatologists studying climatic and atmospheric variability on a global scale. Because of its natural physical properties, snow highly affects the evolution of weather from daily bases to climate on a longer time scale. Changes on snow cover extent has significant influences on radiative balance and energy budget of the Earth. Thus, the accurate observation of the spatial and temporal variability of snow covered area is an important tool for monitoring of the global changes.

Since snow is one of the main water resources, monitoring and estimating the snow cover play an important role in predicting discharges during melting seasons. The ability to characterize snow storage more accurately at the drainage basin scale is crucial for improved water resource management. Snow-water equivalent (SWE), snow cover, and melt onset are critically needed parameters for climate modeling and the initialization of forecasts at weather and seasonal time scales. Snow models may require the following spatially distributed parameters: snow-covered area, grain size, albedo, snow water equivalent, snow temperature profile and meteorological parameters, including solar radiation. In mid-latitudes, snow can be seen continuously in the mountainous terrains. The difficulty in accessibility to perform the measurements at the remote sites makes the use of satellite images and/or aerial photographs in monitoring and estimating the snow parameters more valuable.

The use of snow products retrieved from satellite images in hydrological applications

and to observe the impact of the products are the key issues in Hydrology Satellite Application Facilities (HydroSAF) project, which is financially supported by European Organization for the Exploitation of Meteorological Satellites (EUMETSAT). Turkey is a part of the HydroSAF project, both in developing satellite-derived snow products (snow recognition (SR), effective snow cover and snow water equivalent) for mountainous areas, cal/val of satellite-derived snow products with ground observations and impact studies with hydrological modeling in the mountainous terrain of Europe.

1.1 Purpose and Scope

A pixel value based algorithm has been developed for SR over mountainous areas of Europe. The method is using the satellite images acquired every 15 minutes from geostationary satellite; Meteosat Second Generations (MSG) instrument Spinning Enhanced Visible and Infra-Red Imager (SEVIRI). Reflectance values for VIS 0.6 and NIR 1.6 channels and brightness temperature values for IR 10.8 channel were used in the algorithm. In order to remove solar effect on the IR 3.9 channel, a correction with IR 13.4 has been applied. Discrimination of snow and clouds is implemented using channel difference algorithms for each scene and accumulated statistics of cloud and snow classification are used in determining the daily snow product. In this way, it is possible to distinguish clouds from snow by considering their different spectral characteristics. The algorithm also uses Satellite Application Facility to support Nowcasting and Very Short Range Forecasting's (SAFNWC) cloud products. Current algorithm has been used for generating daily snow maps since September 2006 for Europe. The routine generation includes a certain amount of online recalibration/validation to monitor product quality stability and continuously improve error structure characterization.

The validation of the SR product have been held in three stages. Firstly, a visual interpretation and comparison of SEVIRI SR product with MODIS snow cover product have been applied. In addition, the relationship between the pixels determined as snow by SEVIRI SR product and land cover types have been investigated.

Secondly, a daily comparison of the SEVIRI SR product with the snow cover product produced from single National Oceanic and Atmospheric Administration (NOAA) Advanced Very High Resolution Radiometer (AVHRR/3) image belonging to 19^{th} January 2008 has been performed. Finally, SEVIRI SR product has been validated with measurements gathered from 78 different meteorologic stations distributed over Eastern-Turkey.

1.2 Study Area

In the framework of HydroSAF project a subset domain of SEVIRI which is within 25 °N to 75 °N latitudes and 20 °W to 45 °E longitudes have been used (marked with a red rectangle in Figure 1.1 which is the first color image of the Earth acquired by the MSG-2 satellite on 25 January 2006).

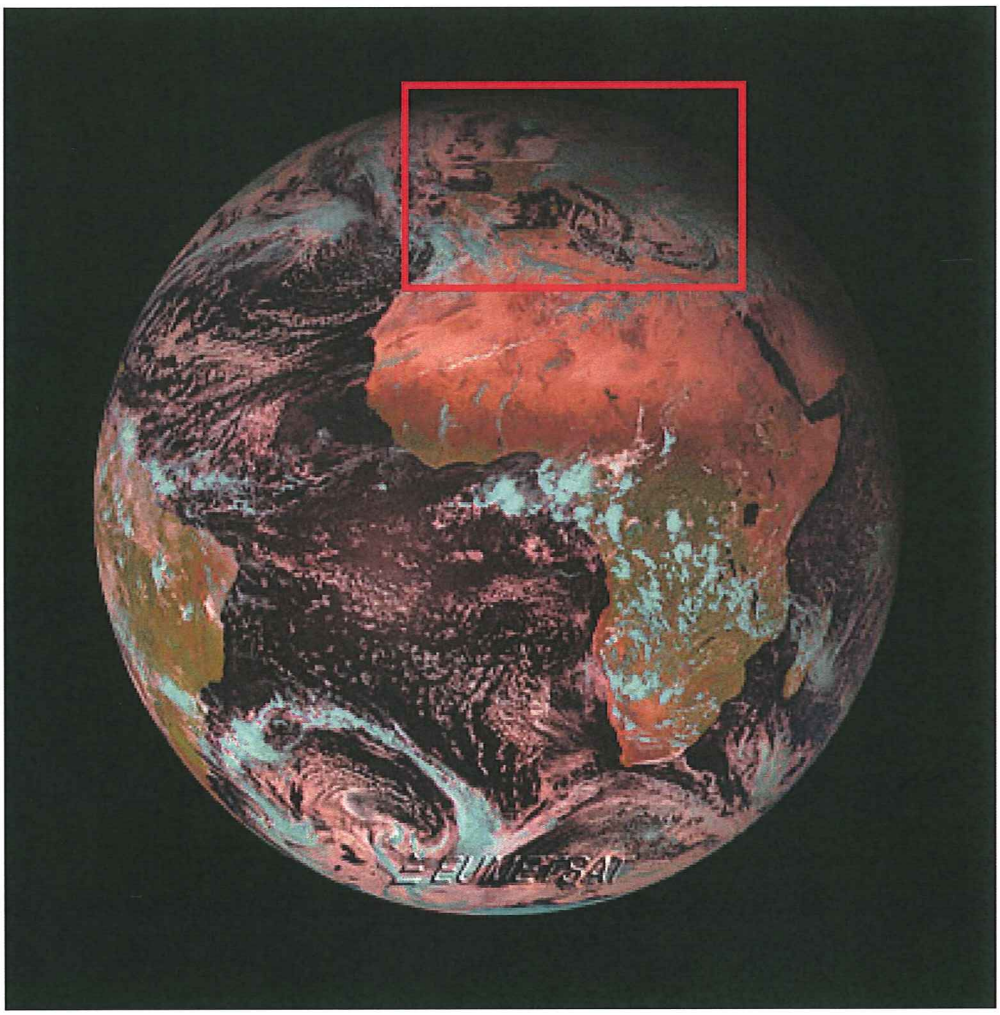

Figure 1.1: The first color image of the Earth acquired by the MSG-2 satellite on 25 January 2006, HydroSAF Project domain within the red rectangle, (`http://www.esa.int/esaEO/SEM1G4NZCIE_index_0.html`, last access:22.07.2008)

CHAPTER 2

REMOTE SENSING OF SNOW

Snow is one of the major water resources in many regions of the world. According to a study made by Shiklomanov (1990), glaciers and permanent snow pack are forming 68.7 % of the total freshwater storage of the world. So, it is quite important to know from both hydrological and meteorological aspects that if there is snow on the ground or not. The spatial distribution of water that is stored as snow is a compulsory input parameter for distributed snow models. Therefore, it is of interest to know the amount of surface area that is covered by snow.

The amount of snow is used to be described by manual field measurements (depth, density) or automatic stations (snow pillows). But these methods have significant disadvantages since they can only describe the snow on specific times and at specific points. Those point measurements are insufficient for determining snow covered area. Moreover, the difficulty in accessibility to perform the measurements at the remote sites makes the use of satellite images and/or aerial photographs in monitoring and estimating the snow parameters more valuable. The satellite images help to describe the snow cover more completely through capturing the temperature and brightness information from surface.

The most efficient way of periodic terrestrial snow cover mapping is by satellite remote sensing since it is possible to obtain up to date and wide areal coverage information for real time operational studies.

2.1 History of Remote Sensing of Snow

There has been several motivation sources for studying snow cover mapping with satellite observations even if it is a difficult task to accomplish. Will to prevent natural disasters like floods or avalanches, accumulation of snow in remote sites that are difficult to access, snow having distinctive properties in some regions of the electromagnetic spectrum, snow being a large scale phenomenon and being an important indicator for global climate change are the most significant motivation sources for detecting snow.

For more than three decades, snow properties from small-basins to continental scales have been measured by satellite remote sensing instruments (Hall and Martinec, 1985). Since snow has a very high albedo in the visible part of the electromagnetic spectrum when compared to other surface covers, the first satellite remote sensing application products were snow covered area maps (Tarble, 1963; Rango and Itten, 1976). Further studies made possible the incorporation of those measurements into snowmelt runoff models (Rango and Martinec, 1979). Later on with the ability of current satellite sensors providing with higher spatial, temporal, and spectral resolutions, the operational snow cover mapping has grown over the following years.

Estimates of snow covered area based on remote sensing have been extracted by various sensors from optical to passive microwave. The earliest remote sensing of snow covered area focused mainly on using multispectral sensors such as the Landsat Thematic Mapper (TM)(Rango, 1980), and the NOAA (Dozier, 1989; Elder et al., 1998). Snow cover mapping has gained more operational abilities after the Earth Observing System (EOS) Terra spacecraft was launched on December 18, 1999, with a complement of five instruments, one of which is the Moderate Resolution Imaging Spectroradiometer (MODIS) instrument. MODIS snow cover products (Hall et al., 2002) significantly improved the performance of operational snow cover mapping by optical remote sensing providing higher spatial resolution. As MSG was launched in 2002 carrying the instrument SEVIRI, the first geostationary satellite that accomodates with channels at all bandwidths that are of use for snow mapping, it became possible to map snow cover in near-real time (de Ruyter de Wildt et al.,

2007). Other than optical remote sensing, microwave sensors also possesses a significant potential for snow/ice cover mapping studies (Rott, 1984; Shi and Dozier, 1997) especially because water and ice represent very different properties in the microwave region of the electromagnetic spectrum. Although microwave sensors have gained much attention over the last decades, snow cover mapping methods based on optical sensors currently provide the most accurate snow-cover estimate for cloud-free situations (Solberg and Andersen, 1994). Images from microwave sensors are more difficult to interpret, and low spatial resolution makes passive microwave sensors suitable primarily for global monitoring (Gupta et al., 2005).

Algorithms to perform snow cover mapping with optical images include unsupervised and supervised classification (Rango and Itten, 1976; Dozier and Marks, 1987; Baumgartner and Rango, 1995; Rosenthal, 1996), thresholds and normalized differences (Dozier, 1989) but those efforts to map snow in binary classifications are problematic for areas showing mixed pixel properties. In order to overcome this mixed pixel problem, linear spectral mixture analysis has been used for deriving sub-pixel snow cover fractions (Nolin and Dozier, 1993), considering the grain size variability of snow as Painter et al. (1998) used a technique in which spectral mixture analysis of optical satellite sensor data incorporating multiple snow endmembers of varying grain size to spectrally characterize the imaged domain and more accurately estimate subpixel SCA. Another well known algorithm for snow cover mapping is the normalized difference snow index (NDSI) that is used for generation of MODIS snow-cover products (Hall et al., 2002). The automated MODIS snow-mapping algorithm uses at satellite reflectances in MODIS bands 4 (0.545 – 0.565 μm) and 6 (1.628 – 1.652 μm) to calculate the NDSI (Hall et al., 1995).

Normalized Difference Snow Index (NDSI)

Snow is characterized by a high reflectance in the visible (0.5 – 0.7 μm) region and a rather strong absorption in the short-wave infrared (SWIR) (1.0 – 3.5 μm) region (Hall et al., 1995; Nolin and Liang, 2000). In contrast, clouds exhibit a near-uniform high reflectance due to non-selective scattering. A spectral band ratio

can enhance features, if there are differences in spectral slopes. Therefore, a ratio of visible/SWIR helps differentiate snow from clouds/other non-snow covered surfaces (Gupta et al., 2005) 2.1.

$$NDSI = \frac{Visible - SWIR}{Visible + SWIR} \tag{2.1}$$

NDSI utilizes the spectral characteristics of snow explained above and is based on the concept of Normalized Difference Vegetation Index (NDVI) used in vegetation mapping from remote sensing data (Dozier, 1989; Hall et al., 1995).

Snow cover mapping has been studied with several multispectral instruments having various spatial, spectral, and temporal resolution such as NOAA AVHRR, EOS MODIS, Terra ASTER, CNES POLDER, and MSG SEVIRI. For continental snow cover mapping studies, geostationary satellites providing with higher temporal resolution are preferred because of their high operational capabilities. In the proceeding section, several previous snow cover mapping studies using MSG-SEVIRI images are summarized.

2.2 Snow Cover Mapping with MSG-SEVIRI

Among many sensor systems presently in orbit (Table 2.1), MSG-SEVIRI instrument is the first geostationary satellite offering all bandwidths useful for snow cover mapping (de Ruyter de Wildt et al., 2007). So, it gives sufficient information for operational studies and near-real time product generation providing required inputs for numerical weather prediction models. Lately, there has been several studies for the purpose of accurate snow cover mapping with MSG-SEVIRI, three of them are summarized below.

Romanov and Tarpley (2006) have developed an automated algorithm to generate maps of snow cover over Europe from Meteosat-8 SEVIRI data. Their snow identification technique is based on satellite observations in the visible, near-infrared, shortwave-infrared and infrared parts of the electromagnetic spectrum including

channels: VIS 0.6 (R1), VIS 0.8 (R2), NIR 1.6 (R3), and IR 10.8 (T9).

Besides spectral criteria, their algorithm utilizes information on temporal variation of the scene temperature and reflectance in order to improve discrimination between snow and clouds in the satellite imagery. They first subject the daily composited image to a threshold-based decision tree unsupervised spectral-based classification, separating the image pixels into snow, snow free land surface and cloud categories as depicted in Figure 2.1.

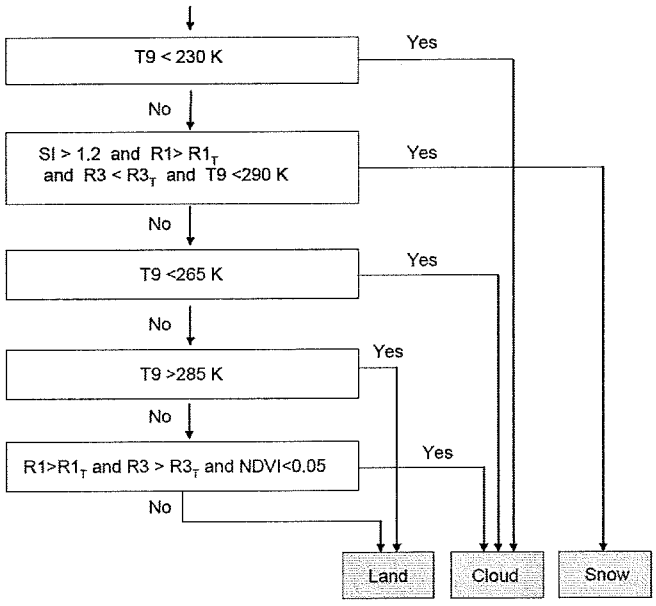

Figure 2.1: Image classification algorithm of Romanov and Tarpley (2006)

Besides the brightness temperature in SEVIRI channel T9, visible and shortwave-infrared reflectance (R1 and R3 respectively), the classification algorithm utilizes a snow index (SI, defined as the ratio R1 / R3). Due to low reflectance of the snow cover in the middle infrared and high reflectance in the visible, the snow index enhances the difference of the spectral response of the snow cover from the response of other surfaces and is thus beneficial for snow detection. They have applied fixed threshold values for SI and T9 channel, whereas for the visible and shortwave

infrared reflectance, the threshold values ($R1_T$ and $R3_T$) were assumed to be location dependent and were defined for every grid cell of the map. They have applied two additional tests based on the land surface temperature climatology and the snow cover climatology in order to further improve the removal of falsely identified snow cover. Satellite derived maps of snow cover distribution have shown a good agreement to snow maps derived interactively at NOAA National Environmental Satellite, Data, and Information Services (NESDIS). Comparison of automated snow maps with surface observation data has shown that snow cover observed on the ground is correctly identified from satellite in about 95 % of all retrievals.

de Ruyter de Wildt et al. (2007) present a snow mapping algorithm that uses change detection in addition to pixel-based spectral classification. The algorithm classifies instantaneous SEVIRI images and can thus produce snow maps in near real-time. They use common satellite observation channels: VIS 0.6, NIR 1.6, IR 3.9, IR 7.3, and IR 10.8. They have used a temporal cloud mask by applying temporal variability tests in order to get rid of moving clouds. Later on they have applied some threshold tests for discriminating snow and snow-free land pixels (Figure 2.2) after removing clouds with cloud mask and temporal cloud classifying tests. For the validation of their final snow cover maps de Ruyter de Wildt et al. (2007) have used three datasets comprising of daily and six days synoptic weather station measurements and another satellite product, the MODIS MOD10A1 daily snow cover product with a resolution of 500 m (Hall et al., 2002). A validation of the results with in situ measurements showed that there are very few false alarms meaning that most of the clouds are detected and hardly any snow is detected where it is not present. The snow cover map also has 73 % of the same pixels with MOD10A1. Currently, their method only produces binary snow cover maps but in the near future they are planing to extend this to fractional snow cover.

Koskinen et al. (2007) have generated a snow recognition model relying on usage of several channels: VIS 0.6, NIR 1.6, IR 10.8, and IR 12.0. The basic principle behind the recognition system is on the different spectral characteristics of snow, clouds and bare ground. The algorithm uses simple difference, ratio and mean thresholds combining the characteristic abilities of different channels. The accuracy of the

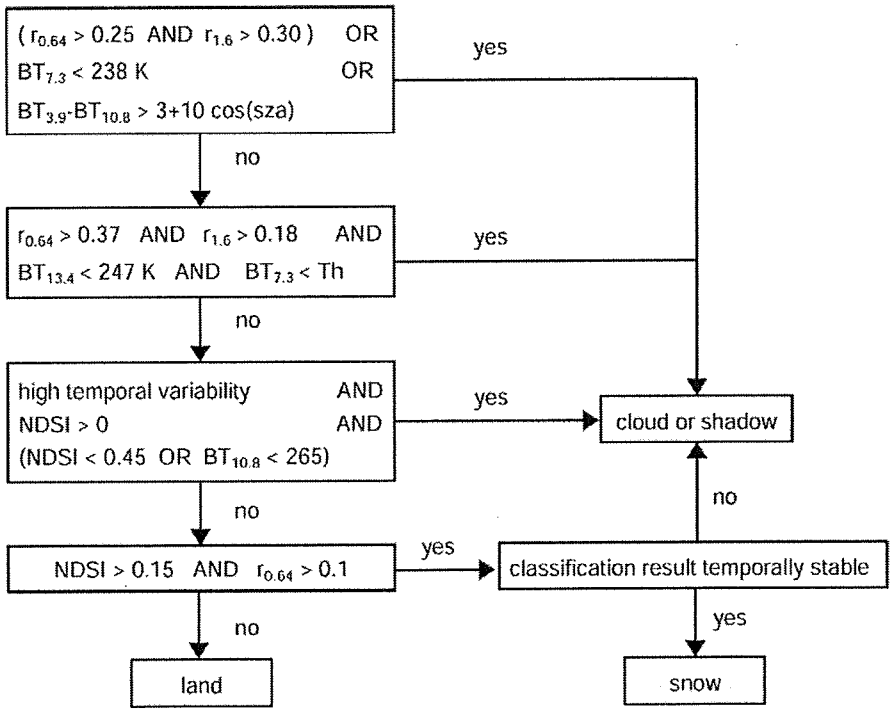

Figure 2.2: Image classification algorithm of de Ruyter de Wildt et al. (2007)

recognition model is yet to be validated with ground measurements.

2.3 Spectral Characteristics of Snow

Snow has a unique reflectance behavior: illuminated by the sun, snow is one of the brightest objects in nature in the optical and near-infrared range ($\sim$ 0.410 μm), but is rather dark in the medium-infrared ($\sim$ 1.5 – 2.5 μm) (Seidel and Martinec, 2004). As can be seen from Figure 2.3 snow shows highly distinctive properties even from ice on the electromagnetic spectrum. Ice is highly transparent in visible wavelengths, so that an increase in grain size has little effect on reflectance. However, in the near-infrared, ice is moderately absorptive (Painter et al., 1998).

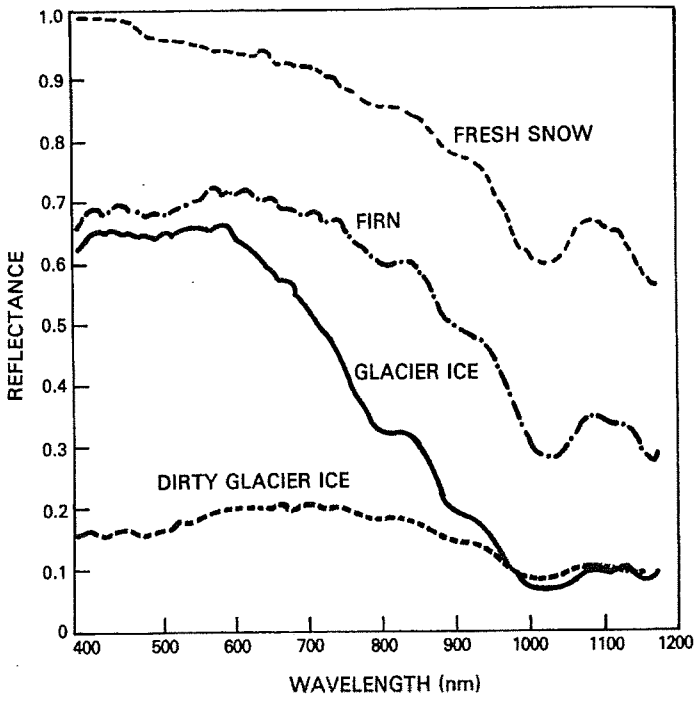

Figure 2.3: Reflectance spectra for different snow and ice surfaces. Adapted from Hall and Martinec (1985)

The spectral reflectance of snow varies with environmental condition, grain size of snow, and time. The spectral reflectance will change especially when meltwater appears and snow crystals metamorphose to coarse grains and density increases (Qunzhu et al., 1983).

2.3.1 Albedo and Grain Size

Albedo is the fraction of solar energy that is reflected back from Earth to space. Since snow has the highest albedo among the other natural surfaces, it has an important effect in change of the Earth's radiation balance. The areal extent of snow cover is likely to be a sensitive indicator of climate change (Gleick, 1987). For calculation of albedo (angularly integrated reflectance), an "equivalent sphere" with the same volume-to-surface ratio as the actual snow grains works well, although such a simplification is possibly inadequate for calculation of the angular details of

the reflectance (Leroux et al., 1998; Warren, 1982).

Grain size is the snow parameter that determines its spectral albedo in the near-infrared wavelengths, while absorbing impurities and, for shallow snow only, snow water equivalence affects its albedo in the visible spectrum (Wiscombe and Warren, 1980). Variation of spectral reflectance of snow depending upon grain size can be seen in Figure 2.4.

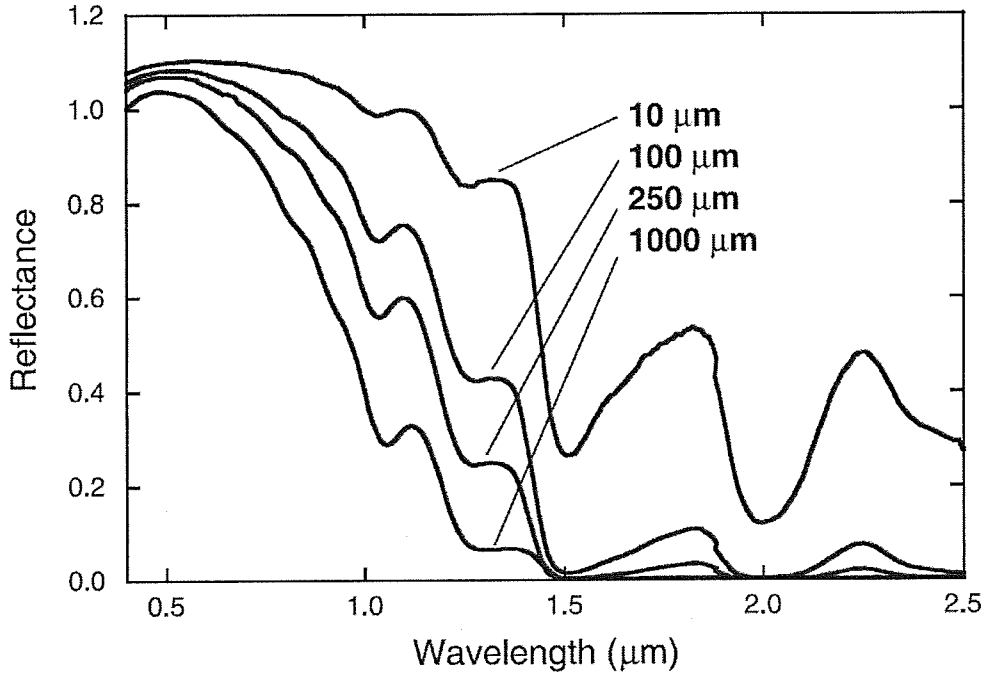

Figure 2.4: Subset of snow spectral library for April 29, 1998 for grain size 10 - 1000 μm. Adapted from Painter et al. (2003)

Table 2.1: Characteristics of common satellites for snow cover mapping (Status: June 2003). Adapted from Seidel and Martinec (2004)

Satellite	Sensors	Spectral bands	Spatial resolution	Repetition rate
Meteosat-7	VIS/IR	3	2.5 km x 2.5 km	0.5 h
Meteosat-8	VIS/IR	12	1 km x 1 km	0.25 h
Meteosat-9	VIS/IR	12	1 km x 1 km	0.25 h
NOAA-14, -16	AVHRR	5	1 km x 1 km	12...24 h
TERRA, AQUA,	MODIS-XS	36	250 m, 500 m, 1000 m	1...18 d
ENVISAT	MERIS	15	300 m x 300 m	35 d
Landsat-4, -5	MSS	4	59 m x 79 m	16 d
	TM	7	30 m x 30 m	
Landsat-7	ETM+	7	30 m x 30 m	16 d
	PAN	1	15 m x 15 m	
SPOT-2, -3, -4	XS	3	20 m x 20 m	26 d
	PAN	1	10 m x 10 m	
			5 m x 5 m	
SPOT-5	XS	3	10 m x 10 m	26 d
IRS-1C	PAN	1	5.8 km x 5.8 km	5...24 d
	LISS-3	4	23 km x 23 km	
IRS-P3	WIFS	3	188 m x 188 m	24 d
IKONOS	XS	4	4 m x 4 m	3 d ...
	PAN	1	1 m x 1 m	
QUICKBIRD-2	XS	4	2.44 m x 2.88 m	3 d ...
	PAN	1	0.61 m x 0.72 m	

CHAPTER 3

DATA

During the development, production, and validation stages of the SEVIRI SR product, both satellite imageries and ground measurements have been used. In this chapter, the satellite data, ground measurements data, and the methodology in retrieving the SEVIRI SR product will be explained.

3.1 Satellite Data

Among many Earth observation satellites, two main Earth observing satellites, MSG and NOAA satellite systems have been used for the purposes of: snow recognition algorithm development, snow recognition product generation and testing of the final product. Firstly, images obtained from MSG SEVIRI satellite have been used for the development of snow and cloud recognition algorithms by multispectral thresholding approach. Secondly, NOAA AVHRR images, considered to have better spatial resolution compared to SEVIRI, have been used for accuracy assessment study of generated products with a better spatial resolution satellite images. All of the satellite data were stored at a dedicated server located at TSMS and served to Middle East Technical University, Civil Engineering Department, Water Resources Laboratory via a file transfer protocol server as illustrated in Figure 3.1. In the following two subsections of Chapter 3, the detailed information about the satellite data used in this study is given.

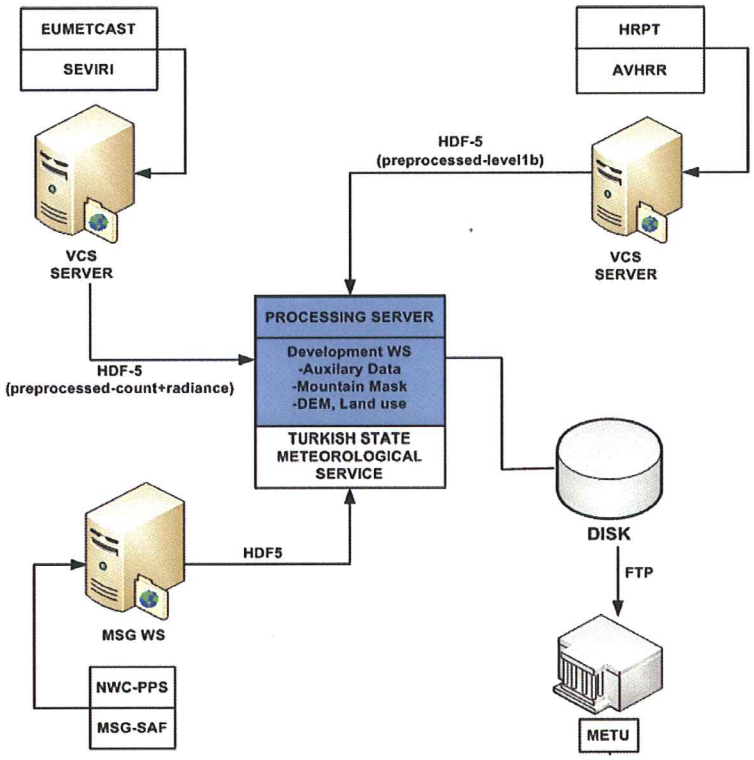

Figure 3.1: The data flowchart of the project

3.1.1 MSG SEVIRI

MSG is a joint project between European Space Agency (ESA) and EUMETSAT and follows up the success of the first generation Meteosat weather satellite series with a larger design boasting higher performance. The first in a planned series of MSG satellites was launched in 2002, entering into service with EUMETSAT in early 2004 and now renamed Meteosat-8. MSG-2 was launched in turn on 21 December 2005, in order to guarantee continuity of service well into the future.

The MSG satellites provide improved information and imagery for weather forecasting as well as other applications such as hydrology, agriculture and environmental studies. The data collected are routinely used for the study of weather and climate change and have proved to be vital in the context of severe weather situations where they help to reduce losses of human life and property. The comparison of spectral,

spatial, and temporal resolutions of the MSG with other well known satellite systems are shown in Figure 3.2 and Figure 3.3.

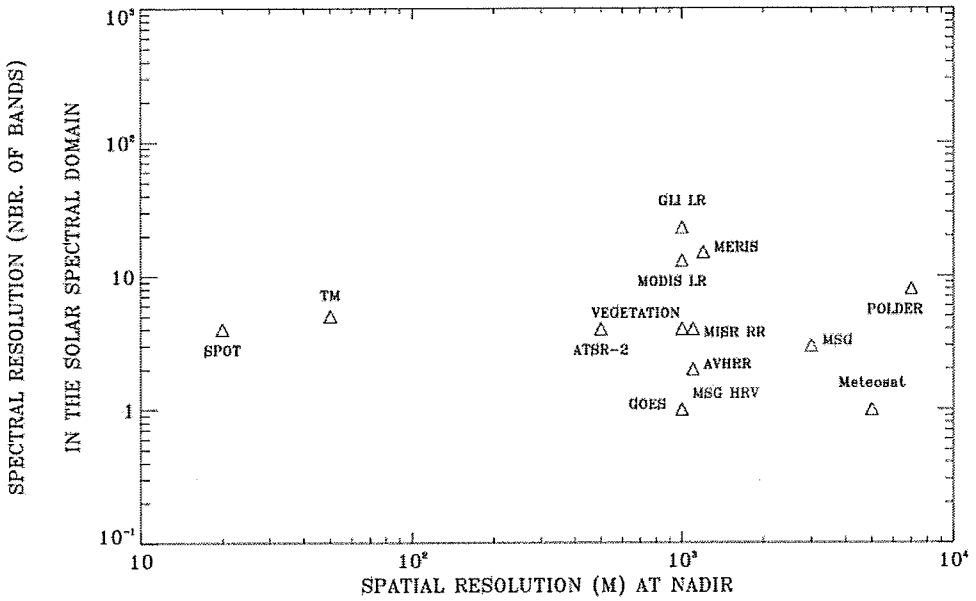

Figure 3.2: Comparison of spatial and spectral resolution of MSG with other well known satellites. Adapted from Cihlar et al. (1999)

MSG-2 (redesignated Meteosat-9) is serving as the prime operational meteorological satellite for Europe. MSG-2 monitors the Earth and its atmosphere from a fixed position in geostationary orbit at 0° longitude, 35 800 km above the Gulf of Guinea off the west coast of equatorial Africa. The satellite previously occupying that position, Meteosat-7, has been moved to 63° East. Meteosat-8 will stay on standby as its "hot" back-up at 3.4 ° West.

SEVIRI is a line-byline scanning radiometer, which provides image data in 12 spectral channels shown in Table 3.1 including four Visible and Near-InfraRed (VNIR) channels, eight InfraRed (IR) channels, and a high resolution visible (HRV) channel. While HRV has 1 km spatial resolution at sub satellite point (SSP), the rest of the channels have 3 km spatial resolution at SSP. The high rate SEVIRI image

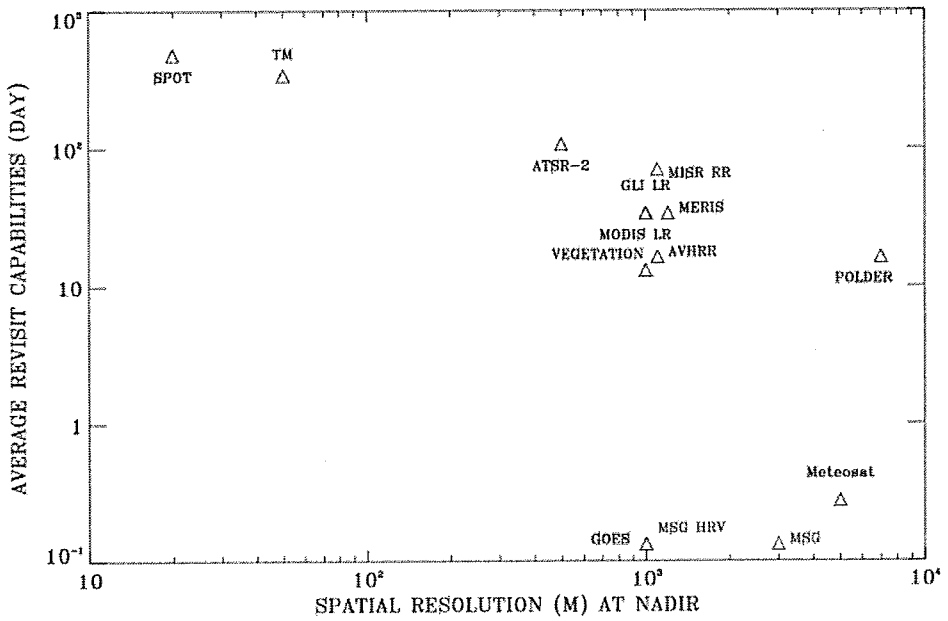

Figure 3.3: Comparison of spatial and temporal resolution of MSG with other well known satellites.Adapted from Cihlar et al. (1999)

data has 15 minutes repeating cycle providing with a high temporal resolution.

Level 1.5 HRIT Data

EUMETSAT, with support from other satellite applications facilities throughout Europe, extracts information from the processed SEVIRI data and turns it into "products" of particular use to meteorologists and climatologists, such as wind field diagrams, maps of upper tropospheric humidity and analysis of cloud shape and height.

For the generation of the snow recognition and cloud recognition products only MSG SEVIRI data have been used. Level 1.5 high rate information transfer (HRIT) data has been received by TSMS from EUMETSAT servers and directed to METU for preprocessing. Level 1.5 data are derived from the Level 1.0 data that is acquired by the MSG satellite and received by EUMETSAT's ground segment. EUMETSAT

Table 3.1: Channel characteristics of SEVIRI

Channel ID	Central Wavelength (μm)	Spectral Band	Primary Objective
VIS 0.6	0.635	0.56 - 0.71	Surface, clouds, wind fields
VIS 0.8	0.81	0.74 - 0.88	Surface, clouds, wind fields
NIR 1.6	1.64	1.50 - 1.78	Surface, cloud phase
IR 3.9	3.90	3.48 - 4.36	Surface, clouds, wind fields
WV 6.2	6.25	5.35 - 7.15	Vapor, high level clouds, atmospheric instability
WV 7.3	7.35	6.85 - 7.85	Water vapor, atmospheric instability
IR 8.7	8.70	8.30 - 9.10	Surface, clouds, atmospheric instability
IR 9.7	9.66	9.38 - 9.94	Ozone
IR 10.8	10.80	9.80 - 11.80	Surface, clouds, wind fields, atmospheric instability
IR 12.0	12.00	11.00 - 13.00	Surface, clouds, atmospheric instability
IR 13.4	13.40	12.40 - 14.40	Cirrus cloud height, atmospheric instability

corrects in real-time each received Level 1.0 image for all radiometric and geometric effects and geolocates it using a standardized projection. The resulting Level 1.5 image consists of Earth-located, calibrated and radiance-linearised information that is suitable for the derivation of meteorological products and other further meteorological processing.

Nominally the full Earth disk is covered for all image channels except HRV. For HRV only half Earth coverage in E-W is provided. The nominal repeat cycle duration providing this Earth coverage is 15 minutes. A visual representation of the full coverage of the Level 1.5 data is given in Figure 3.4.

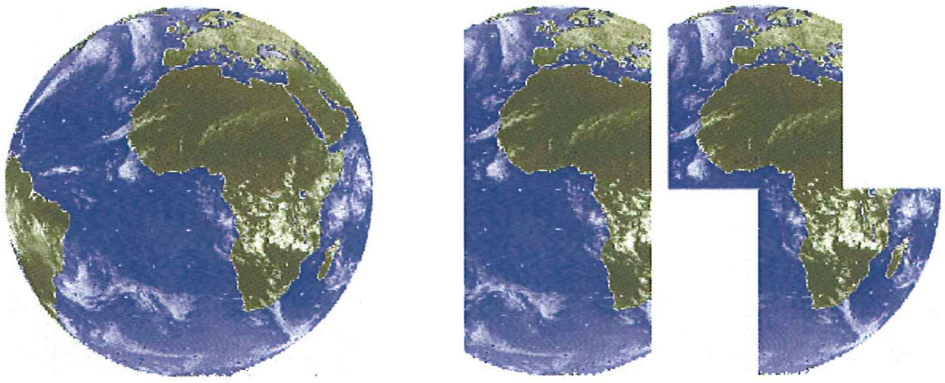

Figure 3.4: Nominal Earth coverage of MSG image channels

For all channels except HRV, the nominal Level 1.5 image size is 3712 lines by 3712 columns (N-S by E-W), the sampling distance defined to be exactly 3 km by 3 km at the sub-satellite point (Fowler, 2006).

MSG SEVIRI Channels

MSG SEVIRI, being the first geostationary satellite sensor provides wide coverage of the electromagnetic spectrum with its 12 spectral channels. A comparison of MSG SEVIRI and several satellite sensors that have been used for snow mapping is given in Figure 3.5.

The spectral channels used for snow cover mapping algorithm development are:

- VIS 0.6
- NIR 1.6
- IR 3.9
- IR 10.8

Most of the SEVIRI spectral channels were build upon the information of inheritance from other satellites which give a great advantage that the operational user

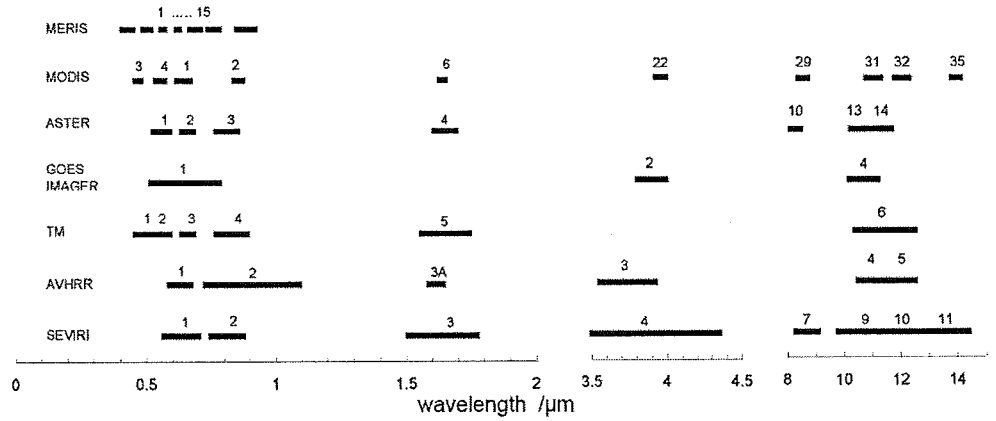

Figure 3.5: A comparison of the several satellite sensors that have been used for snow mapping. Only channels that are relevant to snow mapping are shown. Adapted from de Ruyter de Wildt et al. (2007)

community can easily use existing know-how to make use of SEVIRI radiance observations. The description and inheritance of the spectral channels used within the algorithm development can be summarized as follows:

VIS 0.6: The characteristics of this visible channel are well known from the similar channels of the AVHRR instrument flown on NOAA satellites. Most of the surfaces present relatively low reflectances in this channel other than snowy, sun glint-affected, or deserted environments. This causes high contrasts to clouds which often display albedos around 0.8 μm or more in this channel (Reuter, 2005). Accordingly, this channel is the most suitable one in order to be used for detection of clouds because of their high reflectance. Under utilization of this channel, the detection of low stratus clouds which show minor contrasts in the thermal channels can be improved significantly. Channels coinciding in this region of spectrum are commonly used for cloud detection (Arking and Childs, 1984; Rossow and Garder, 1993) and retreival of cloud optical thickness (Nakajima et al., 1991; King et al., 2007).

NIR 1.6: The reflectivity of clouds is considerably higher at this channel compared to the reflectivity of snow. Ice has a significantly higher radiation absorption capacity than water at 1.6 μm. Water clouds with their high reflectivity, can be

discriminated from snow much better than ice clouds. Consequently, this channel is very useful to make discrimination between snow and low water clouds (Ackerman et al., 1998), ice and water clouds, and also provides aerosol information. NIR 1.6 channel is also useful for deriving cloud optical thickness and cloud droplet effective radius (King et al., 1997).

IR 3.9: Also well known from AVHRR. This is the only SEVIRI channel, whose signal is affected from both solar radiation and thermal radiation of the earth. Therefore, its interpretation is different at daytime and nighttime. Primarily used for detection of low cloud and fog at night like (Cermak and Bendix, 2008) and for the determination of cloud properties, but also useful for measurement of land and sea temperatures at night and the detection of wildfires (EUMETSAT, 2005; Calle et al., 2006). When using only thermal information it is hard to distinguish low clouds from surfaces with the same temperature. In order to overcome this problem IR 3.9 provides major additional information both at daytime and nighttime.

IR 10.8: One of the well-known (from AVHRR) split-window thermal infrared channels. Temperature of the clouds and surface information can be obtained from this channel. By using together with other thermal channels like IR 12.0 or IR 13.4, it is possible to reduce atmopsheric effects when measuring surface and cloud top temperatures. Due to Mie scattering properties, the penetration depth of clouds in this channel is comparatively low. Consequently, this channel is suitable for detecting clouds due to their temperature which is generally lower than the temperature of the surface beneath. Low brightness temperatures measured in this channel as well as high differences to the estimated clear sky brightness temperatures give an excellent indication for the presence of clouds (EUMETSAT, 2005). Nevertheless, the discrimination of fog or low stratus clouds and surface only from this channel is often not possible because of very low contrasts (Ernst, 1975).

Description of the Domain

MSG SEVIRI instrument continuously monitors the whole hemisphere. Nominal coverage includes the whole of Europe, all of Africa and locations at which the

elevation to the satellite is greater than or equal to 10°. MSG normalized pixel area can be seen in Figure 3.6.

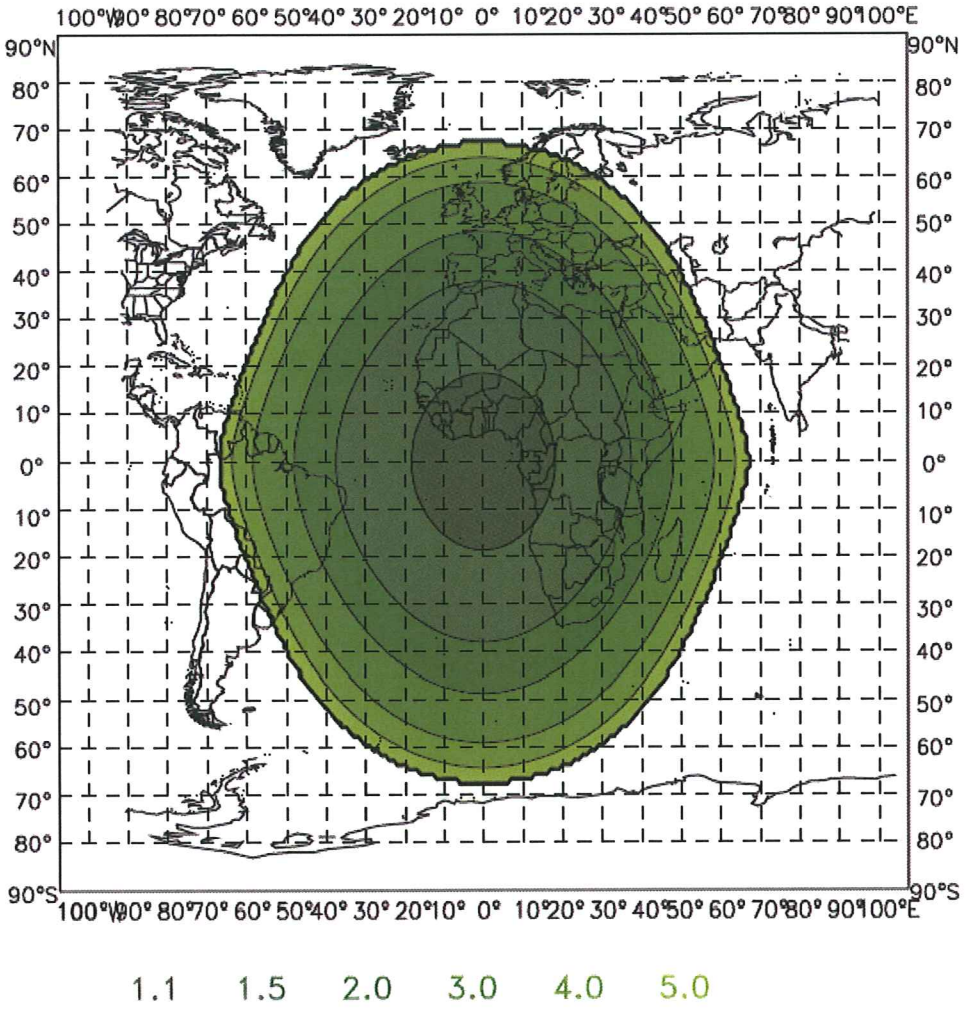

Figure 3.6: MSG normalized pixel area. The result is shown in an equidistant cylindrical projection. Adapted from Cihlar et al. (1999)

SEVIRI Calibration

Accurate calibration of data is essential to the successful extraction of quantitative information from satellite data, because the extraction relies on numerical models that relate the satellite signal to the parameter of interest. Calibration errors will thus very probably be translated into significant errors in the information obtained. In the case of land observations, the importance of calibration is further underlined by the often small dynamic range of the radiometer signal from the land biosphere, and the need to discern the part of the signal attributable to the parameter of interest. Since the calibration requirement is common to all quantitative applications of satellite data, its implementation is of fundamental importance to the success of the satellite mission. Both absolute and relative calibration are important. Absolute calibration allows measurements from one satellite sensor to be compared with another. Relative calibration will negate the impact of a bias in calibration on specific derived products. This can be achieved through product validation campaigns or other quality control measures (Schmetz et al., 2002).

Solar Channel Calibration: As no on-board calibration device is available for the solar channels of MSG/SEVIRI, their calibration has to rely on a vicarious method. This method relies on radiative transfer modelling over bright desert and clear ocean sites. The choice of this method has been driven by the need to fulfil the accuracy and precision requirements of the MSG operational ground segment during the entire duration of the mission (more than 12 years). Radiative transfer simulations are performed with the 6S code (Tanre et al., 1990), using a data set of surface and atmospheric properties. This data set is used to simulate SEVIRI observations accounting for the exact viewing and illumination conditions as well as the spectral characteristics of the instrument. The duration of the MSG mission prohibits the continuous characterization of a limited number of targets with ground observations. The proposed strategy relies therefore on the definition of a large number of stable targets for which surface properties are estimated once and for all. The accuracy and precision of these calculated radiances are estimated comparing simulations with calibrated observations acquired by space borne instruments. An

operational algorithm, named SEVIRI Solar Channel Calibration (SSCC), has been developed to ensure a routine calibration of the solar channels. First results show that SEVIRI solar channels can be calibrated with an estimated accuracy ranging from 4 – 6 %, at the 95 % confidence level, according to the band.

Thermal Infrared Channel Calibration: In the current MSG calibration scheme, the SEVIRI thermal channels can be seen as a radiance thermometer. The calibrated radiance is provided as a spectral blackbody radiance. Detailed information about some of the methods used for vicariuos calibration of previous Meteosat satellites can be found in Govaerts et al. (2001); Kriebel and Amann (1993).

3.1.2 SAFNWC Cloud Products

During the development of snow recognition algorithm, a combination of the cloud products of Satellite Aplication Facility to support to Nowcasting and Very Short Range Forecasting (SAFNWC) have been used as the cloud detection part of the main algorithm as a replacement of our own previously developed cloud detection algorithm product.

The EUMETSAT SAFNWC has been hosted since 1997 by the Spanish Meteorological Institute (INM). The objective of this SAF is to develop an operational software package to produce 12 products (aiming to support nowcasting applications) using data from the future EUMETSAT MSG and EUMETSAT Polar System (EPS) meteorological satellites. Four weather services are involved in this SAF: INM (Spanish weather service), SMHI (Swedish weather service), ZAMG (Austrian weather service) and Meteo-France.

The Centre de Meteorologie Spatiale (CMS) of Meteo-France is responsible for the development and scientific maintenance of software modules that allow to extract 3 cloud parameters: CMa: cloud mask, CT: cloud types, CTTH: cloud top temperature and height from MSG SEVIRI imagery over European areas.

In the following two subsections the details of two SAFNWC cloud products (CMa and CT) that we have utilized during snow recognition algorithm development have been given.

Cloud Mask (CMa):

The cloud mask (CMa), developed within the SAFNWC context, aims to support nowcasting applications, and additionally the remote sensing of continental and oceanic surfaces. The CMa allows identifying cloud free areas where other products (total or layer precipitable water, land or sea surface temperatures, snow/ice cover delineation) may be computed. It also allows identifying cloudy areas where other products (cloud types and cloud top temperature/height) may be derived.

The central aim of the CMa is therefore to delineate all cloud-free pixels in a satellite scene with a high confidence. In addition, the product provides information on the presence of snow/sea ice, dust clouds and volcanic plumes. A sample CMa product is given in Figure 3.7. The decription of each pixel value of the CMa product is also given in Table 3.2.

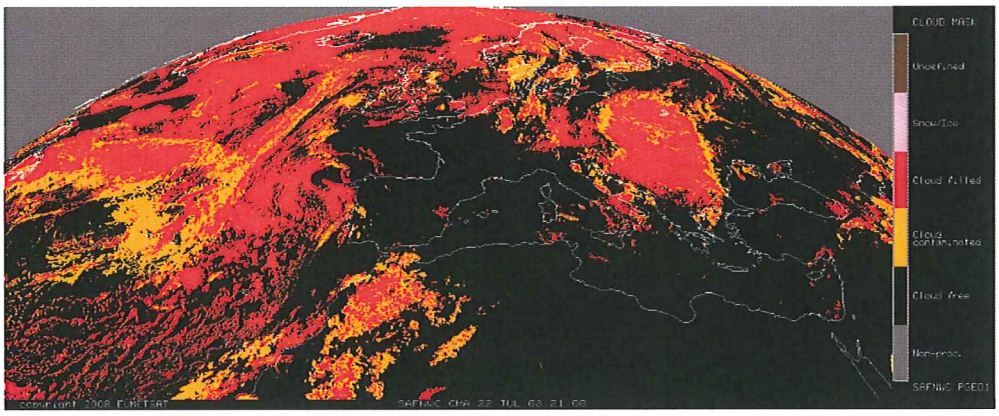

Figure 3.7: A sample CMa product generated for 22 July 2008

The algorithm is based on multispectral threshold technique applied to each pixel

Table 3.2: The description of CMa product pixel values

Pixel Value	Category	Description
0	Non-processed	containing no data or corrupted data
1	Cloud Free	no contamination by snow/ice covered surface; no contamination by clouds but contamination by thin dust/volcanic clouds not checked
2	Cloud contaminated	partly cloudy or semi-transparent May also include dust clouds or volcanic plumes
3	Cloud filled	opaque clouds completely filling the FOV, may also include thick dust clouds or volcanic plumes
4	Snow/ice contaminated	
5	Undefined	has been processed but not classified due to known separability problems

of the image. A first process allows the identification of pixels contaminated by clouds or snow/ice. It consists in a series of tests applied to various channels combination for each pixels of the current slot. This is complemented by an analysis of the temporal variation (on a short period of time: 15 minutes) of some spectral combination of channels (to detect rapidly moving clouds) and a specific treatment combining temporal coherency analysis and region growing technique (to improve the detection of low clouds).

The characteristics of the first set of tests are summed up below:

- The tests, applied to land or sea pixels, depend on the solar illumination and on the viewing angles (daytime, night-time, twilight, sunglint)
- Most thresholds are determined from satellite-dependent look-up tables using as input the viewing geometry (sun and satellite viewing angles), NWP forecast fields (surface temperature and total atmospheric water vapour content) and

ancillary data (elevation and climatological data). These look-up tables have been prepared off-line using radiative transfer models (RTTOV (Eyre, 1991) for infrared channels, 6S (Tanre et al., 1990) for solar channels).The thresholds are computed at a spatial resolution defined by the user as a number of SEVIRI infra-red pixels. Some thresholds are empirical, constant or satellite-dependent values.

- The quality of the cloud detection process is assessed by analysing how close the measurements and the thresholds are from each other.

This first process allows to determine the cloud cover category of each pixel (cloud-free, cloud contaminated, cloud filled, snow/ice contaminated or undefined/non processed) and compute a quality flag on the processing itself. Moreover, the tests that have allowed the cloud detection are stored.

A second process, allowing the identification of dust clouds and volcanic ash clouds, is applied to all pixels (even already classified as cloud-free or contaminated by clouds). The result is stored in the dust cloud and volcanic ash cloud flags

Cloud Type (CT):

The cloud type (CT), developed within the SAFNWC context, mainly aims to support nowcasting applications. The main objective of this product is to provide a detailed cloud analysis. It may be used as input to an objective meso-scale analysis (which in turn may feed a simple nowcasting scheme), as an intermediate product input to other products, or as a final image product for display at a forecasters desk. The CT product is essential for the generation of the cloud top temperature and height product and for the identification of precipitation clouds. Finally, it is also essential for the computation of radiative fluxes over sea or land, which are SAF Ocean & Sea Ice products.

The CT product therefore contains information on the major cloud classes : fractional clouds, semitransparent clouds, high, medium and low clouds (including fog) for all the pixels identified as cloudy in a scene. A second priority (not implemented

in the current version) is the distinction between convective and stratiform clouds, and the identification of clouds for which the top mainly consists of water droplets. The description of each pixel value of the CT product is given in Table 3.3 and a sample CT product is given in Figure 3.8.

Table 3.3: The description of CT product pixel values

Pixel Value	Category
0	non-processed
1	cloud free land
2	cloud free sea
3	land contaminated by snow
4	sea contaminated by snow/ice
5	very low and cumuliform clouds
6	very low and stratiform clouds
7	low and cumuliform clouds
8	low and stratiform clouds
9	medium and cumuliform clouds
10	medium and stratiform clouds
11	high opaque and cumuliform clouds
12	high opaque and stratiform clouds
13	very high opaque and cumuliform clouds
14	very high opaque and stratiform clouds
15	high semitransparent thin clouds
16	high semitransparent meanly thick clouds
17	high semitransparent thick clouds
18	high semitransparent above low or medium clouds
19	fractional clouds (sub-pixel water clouds)
20	undefined (undefined by CMa)

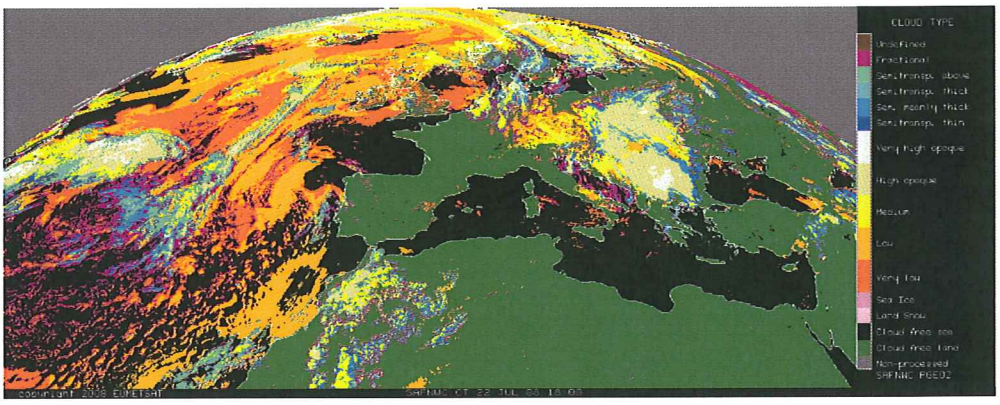

Figure 3.8: A sample CT product generated for 22 July 2008

The CT algorithm is a threshold algorithm applied at the pixel scale, based on the use of CMa and spectral and textural features computed from the multispectral satellite images and compared with a set of thresholds. The set of thresholds to be applied depends mainly on the illumination conditions, whereas the values of the thresholds themselves may depend on the illumination, the viewing geometry, the geographical location and NWP data describing the water vapour content and a coarse vertical structure of the atmosphere.

The CT classification algorithm is based on the following approach:

- Main cloud types are separable within two sets: the fractional and high semitransparent clouds, from the low/medium/high clouds. These two systems are distinguished using spectral features: T10.8 μm - T12.0 μm, T3.9 μm - T10.8 μm (in night-time conditions only), R0.6 μm (in day-time conditions only), and textural features (variance T10.8 μm coupled to variance R0.6 μm in daytime conditions) .

- Within the first set, the fractional and high semitransparent are separated using either their T8.7 μm - T10.8 μm brightness temperature differences, but also their R0.6 μm visible reflectance (in daytime conditions only).

- The remaining categories are distinguished through the comparison of their T10.8 μm to NWP forecast temperatures at several pressure levels, T10.8 μm

- T7.3 μm being used to make sure that low clouds are not wrongly classified as medium cloud in case strong low level thermal inversion.

- No separation between cumuliform and stratiform clouds is performed in the current version of CT.

- No cloud phase flag is available in the current version of CT.

(`http://www.meteorologie.eu.org/safnwc/`, last access:22.07.2008)

3.1.3 NOAA

NOAA and National Aeronautics and Space Administration (NASA) jointly administer the civilian polar orbiting spacecraft system for the United States. The normal suite of instruments onboard the NOAA KLM series includes the following instruments: AVHRR/3, HIRS/3, AMSU-A and -B, SEM-2, DCS/2, SARSAT and sometimes SBUV/2.

Validation of MSG SEVIRI SR product with a higher spatial resolution satellite sensor has been made with the SR product generated from a single NOAA AVHRR/3 data for the date 19^{th} January 2008. A detailed description of AVHRR/3 instrument is provided in the subsection below.

AVHRR/3:

The Advanced Very High Resolution Radiometer/3 (AVHRR/3) is a multipurpose imaging instrument used for global monitoring of cloud cover, sea surface temperature, ice, snow and vegetation cover characteristics. The AVHRR/2 version of the instrument is currently flying on the NOAA/TIROS-N series of spacecraft in a five-channel version. The spectral channels (Table 3.4) of AVHRR/3 are not exactly the same as AVHRR/2, and include an additional channel 3a in the near infrared (NIR). AVHRR/3 has 6 spectral channels between 0.63 and 12.00 micrometers: 3 in the visible/near infrared and 3 in the infrared. Channel 3 is a split channel. Channel 3a is in the solar spectral region (1.6 μm) whereas Channel 3b operates in

the infrared around 3.7 μm. Channel 3a will be operated during the daytime portion of the orbit, and 3b will be operated during the night-time portion of the orbit. The transition from Channel 3a to 3b and vice versa will be done by telecommand (Ackermann, 2004).

Table 3.4: Summary of AVHRR/3 Spectral Channel Characteristics

Channel Number	Resolution at Nadir	Wavelength (μm)	Typical Use
1	1.09 km	0.58 - 0.68	Daytime cloud and surface mapping
2	1.09 km	0.725 - 1.00	Land-water boundaries
3a	1.09 km	1.58 - 1.64	Snow and ice detection
3b	1.09 km	3.55 - 3.93	Night cloud mapping, sea surface temperature
4	1.09 km	10.30 - 11.30	Night cloud mapping, sea surface temperature
5	1.09 km	11.50 - 12.50	Sea surface temperature

AVHRR/3 is an across track scanning system with a scan range of $\pm 55.37°$ with respect to the nadir direction. The field of view (IFOV) of each channel is approximately 1.3 milliradians (0.0745 deg) leading to a square instantaneous field of view size of 1.08 km at nadir for a nominal altitude of 833 km. The scanning rate of 360 scans per minute is continuous (1 scan every 1/6 second). There are 2048 Earth views per scan and per channel for a swath width of about $\pm$ 1447 km (sampling time of 0.025 ms). The sampling angular interval is close to 0.944 milliradians (0.0541 deg). The distance between two consecutive scans is approximately equal to 1.1 km.

Calibration: The AVHRR/3 calibration is different for the visible and the IR channels:

- There is no on-board calibration for the visible channels (channels 1 and 2) and channel 3a. The calibration coefficients for these channels are determined before launch. The calibration function on the ground can act on the visible calibration (e.g. by vicarious calibration).
- The calibration of the infrared channels (channels 3b, 4 and 5) is performed by viewing an internal black body and the cold space. The internal rotating scan mirror views the deep space or a thermal calibration source at each rotation: a minimum of 55 scan lines is needed to obtain a complete set of calibration coefficients. The temperature of the internal black body is measured by four platinum resistance thermometers (PRTs)(Ackermann, 2004).

3.2 Terrestrial Measurements of Snow

Ground information has been defined as information derived from ground data and surveys to support interpretation of remotely sensed data (Seidel and Martinec, 2004). Point measurements of snow depth from various weather observation stations have been used for the accurate validation of the snow recognition product obtained from satellite observations. These terrestrial measurements of snow depth were obtained from: synoptic weather stations, automated weather observation stations (AWOS), and big climate stations. In the following subsections, information about the ground stations are given.

3.2.1 Synoptic Weather Stations

Synoptic measurements are surface weather observations, made at periodic times (usually at 3-hourly and 6-hourly intervals specified by the World Meteorological Organization), of sky cover, state of the sky, cloud height, atmospheric pressure reduced to sea level, temperature, dew point, wind speed and direction, amount of

precipitation, hydrometeors and lithometeors, and special phenomena that prevail at the time of the observation or have been observed since the previous specified observation (`http://nsidc.org/arcticmet/glossary/synoptic_weather_ob.html`, last access:22.07.2008).

Snow depth measurements from four different synoptic weather stations as listed in Table 3.5 have been used for the validation purpose of SR product.

Table 3.5: List of synoptic weather stations used for validation

Name	Elevation (m)	Latitude (°)	Longitude (°)
Erzincan	1154	39.70	39.52
Kars Meydan	1795	40.57	43.10
Ferit Melen Meydan	1665	38.27	43.19
Erkilet	1053	38.49	35.26

3.2.2 Automated Weather Observation Stations (AWOS)

AWOS are automated devices that take measurements hourly or more frequently of surface atmospheric pressure; near surface air temperature and humidity; snow depth; near surface wind velocity; precipitation type, rate and amount; visibility; weather conditions; cloud type and amount. Stations stay operational 24 hours a day, 7 days a week.

Snow depth measurements from four different AWOS as listed in Table 3.6 have been used for the validation purpose of snow recognition product.

3.2.3 Big Climate Stations

Big climate stations can be considered as bigger synoptic weather stations since they run on similar basis but measure more parameters than synoptic weather stations.

Table 3.6: List of AWOS used for validation

Name	Elevation (m)	Latitude (°)	Longitude (°)
Güzelyayla	2065	40.12	41.28
Ilıca	2094	39.88	41.07
Dumlu	2666	40.14	41.33
Palandöken	2937	38.80	41.29

They traditionally make three manual observations per day. Observations specially related to rainfall and snow are made once a day at precipitation stations.

Snow depth measurements from 70 different big climate stations distributed mainly over Eastern-Turkey have been used for the validation purpose of SR product. Average elevation of those seventy stations is 1308 meters where lowest station is at 529 meters at Turhal having ID of 17683, and highest station is at 2400 meters at Başkale having ID of 17880. Information for some of the big climate stations are listed in Table 3.7. Complete list of big climate stations is given in Appendix A

Table 3.7: List of some of the big climate stations used for validation

Name	Elevation (m)	Latitude (°)	Longitude (°)
Kars	2102	40.33	42.57
Erzurum Meydan	1758	39.95	41.17
Varto	1650	39.17	41.45
Palu	1000	38.72	39.97

3.3 Verification Metrics

Some statistical scores mostly used for forecast verification, like Probability of detection (POD), have been used for the verification of the satellite products with

ground observations in validation part of the study (5.3). To verify a dichotomous (yes/no) product, like the SR product discussed in this study giving "snow" or "not snow" results, one should start with a contingency table (Table 3.8) that shows the frequency of "yes" and "no" occurrences.

Table 3.8: Contingency table

		Ground	Observations
		Yes	No
Satellite	Yes	a (hits)	b (false alarms)
Product	No	c (misses)	d (correct negatives)

A large variety of categorical statistics can be computed from the elements in the contingency table to describe particular aspects of product performance. The ones listed below were used for validation of the SR product.

Bias: The difference between the mean of the forecasts and the mean of the observations. Could be expressed as a percentage of the mean observation. Also known as overall bias, systematic bias, or unconditional bias. For categorical forecasts, bias (also known as frequency bias) is equal to the total number of events forecast divided by the total number of events observed.

$$Bias = \frac{(a+b)}{(a+c)} \tag{3.1}$$

Probability of Detection (POD): For categorical forecast, the number of hits divided by the total number of events observed. A measure of discrimination.

$$POD = \frac{a}{(a+c)} \tag{3.2}$$

False Alarm Ratio (FAR): For categorical forecast, the number of false alarms divided by the total number of events forecast. A measure of reliability.

$$FAR = \frac{b}{(a+b)} \tag{3.3}$$

Threat Score (TS): Also known as critical success index (CSI). It measures the fraction of observed and/or forecast events that were correctly predicted.

$$TS = \frac{a}{(a+b+c)} \tag{3.4}$$

3.4 Mountain Mask

Since the developed algorithm aims to generate snow cover maps over mountainuos terrain, a mountain mask (Figure 3.9) for Europe has been produced and inserted as a layer into the snow cover mapping algorithm targeting the snow over mountains. Three main criteria have been applied while the production of the mountain mask from a digital elevation model (DEM) which has 1 km resolution. Those three criteria can be listed as:

- Mean DEM $\geq$ 2000m OR
- STD slope $\geq$ 2 degree AND Mean DEM $\geq$ 700 m OR
- Mean DEM $\geq$ 500 m and Range $\geq$ 800 m

The pixels satisfying these three criteria were flagged as "mountain", and the rest of the pixels other than water were flagged as "flat land".

3.5 Digital Elevation Model

GTOPO DEM as shown in Figure 3.10 is a digital elevation model (DEM) having 1 km spatial resolution. It was obtained from Eurosat/GISCO and it has been used

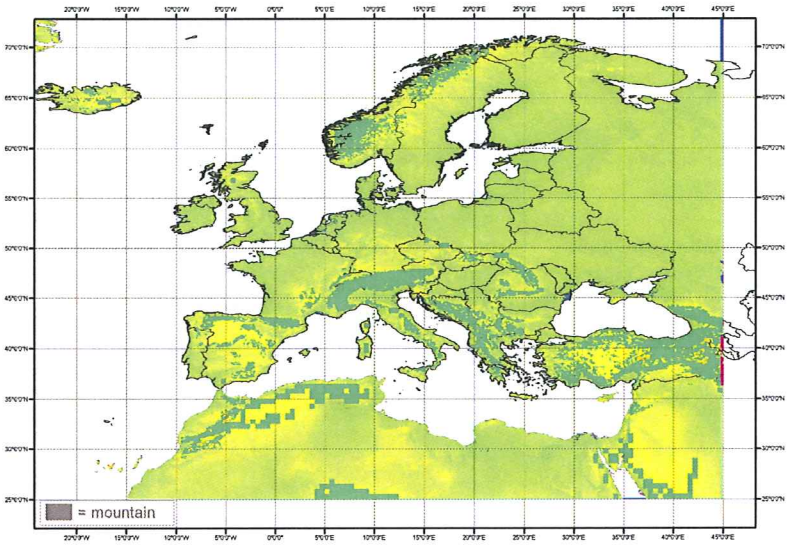

Figure 3.9: The mountain mask for Europe domain

for acquiring elevation values of classified pixels for the comparison of SEVIRI and AVHRR/3 SR products in 5.2.2.

3.6 Land Cover Types

There are several global land cover products available such as MODIS global land cover and GLOBCOVER product of ENVISAT. At operational level, all these products are not in high quality. In this study GLC 2000, 1 km resolution, SPOT vegetation sensor derived land cover product is used (Giri Chandra, 2005). This product is released by Joint Research Center of European Commission. GLC 2000 has 6 forest classes originally, but it has been narrowed down to 3 main forest classes as: evergreen, deciduous, and mixed forest as can be seen in Figure 5.1.

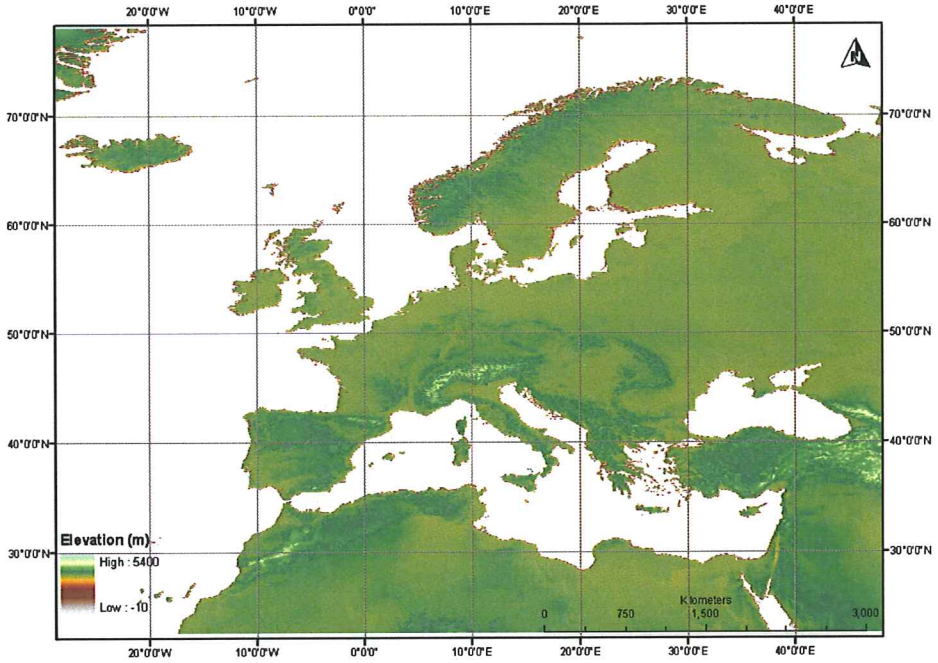

Figure 3.10: GTOPO DEM

CHAPTER 4

METHODOLOGY

For the proposed snow recognition algorithm, spectral thresholding methods were applied on sub pixel scale of SEVIRI image. During algorithm development, some spectral threshold tests that are common in use have been considered (Dozier, 1989; Baum and Trepte, 1999; Hall et al., 2002; de Ruyter de Wildt et al., 2007). The main idea was using the different spectral characteristics of cloud, snow and land. Discrimination of snow and cloud was the most challenging part of snow recognition algorithm development. Before going into further investigation for snow pixels, discrimination of cloud has been done and thereafter only cloud free pixels considered for snow and land discrimination.

4.1 Cloud Detection Algorithm

In snow cover mapping studies, main confusion appears at the stage of snow and cloud discrimination. Snow and clouds have some common spectral characteristics. As can be seen in Figure 4.1 both snow and cloud have similar spectral characteristics in the visible part of the electromagnetic spectrum. Thus, eliminating the effect of clouds is the key in determining snow covered area.

For cloud detection, basic ratio thresholding methods have been used, depending on different behavior of clouds from snow on Channel 1 (VIS 0.6), Channel 3 (NIR 1.6) and Channel 9 (IR 10.8) combinations of SEVIRI data. Cloud detection and extraction part of the SR algorithm have managed to distinguish most of the cloud

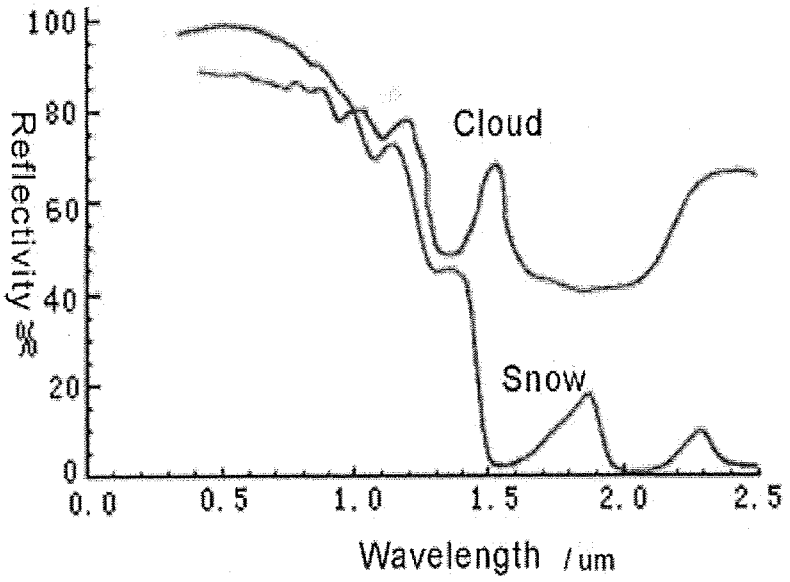

Figure 4.1: Spectral reflectivities of clouds and snow. Adapted from Zhang et al. (2008)

types with threshold ratio and difference methods. The threshold values used in algorithms were determined empirically. On Channel 1, both the surface snow and clouds give high reflectance which helps to separate them from land pixels. Channel 3 has often been used for distinguishing clouds from snow (Hall et al., 1995) because clouds give high reflectance on Channel 3 while snow gives low reflectance. Channel 9 has been used to overcome the possible ambiguity between snow and very cold clouds like cirrus clouds discrimination (Baum and Trepte, 1999).

In the developed algorithm reflectance values calculated from radiances have been used instead of land surface temperatures obtained by using radiative transfer models (RTM). RTMs have not been used since they do not consider the atmospheric sphericity and do not work efficiently on solar zenith angles (sza) over 70 ° which are common angles for snow cover observations during winter (de Ruyter de Wildt et al., 2007). Instead of using RTMs for the cloud detection algorithm and slowing down the real-time SR product generation by overburdening the process, cloud products of another SAF project have been used. The SAFNWC cloud products are generated in real time and RTMs have been used in the generation (Derrien

and Le Gleau, 2005). The purpose of introducing cloud products of SAFNWC is increasing the reliability of the SR algorithm, but the developed cloud detection algorithm kept working as a by-pass line in case of any problem on SAFNWC cloud product generation, to be on the safe side. In order to test the developed cloud detection product before continuing with further classification study for surface snow cover, an accuracy assessment test has been applied with the SAFNWC's CMa product while the main purpose of the CMa is to delineate all cloud-free pixels with a high confidence (Derrien and Le Gleau, 2005).

The baseline algorithm was applied to the image acquired on 19^{th} September 2007 at 09:00 am, and the Cloud Mask (CMa) product of SAFNWC was also determined for the same time increment as in Figure 4.2. In the accuracy assessment 256 points with stratified random distribution were generated. The overall accuracy was obtained as 89.06 % as can be seen from Table 4.1.

Table 4.1: Confusion matrix for accuracy assessment test of cloud product with SAFNWC CMa product on 19^{th} September 2007

Class	Reference Totals	Classified Totals	Numbers Correct	Producers Accuracy	Users Accuracy
Cloud	86	86	72	83.72 %	83.72 %
Land	170	170	156	91.76 %	91.76 %

The general strategy of SAFNWC cloud products is to first detect clouds with the CMa and then classify them using the Cloud Type (CT) module. The well agreement of the tested cloud masking product and CMa product of SAFNWC has been observed by accuracy assessment tests. But CMa product does not cover the contaminated cloud pixels (partially cloud covered, neither clear sky nor full cloud), then a combination of CMa and CT products as the cloud detection part of the SR algorithm has been developed. Since the main objective of CT is to provide a detailed cloud analysis providing 20 different classes, a combination of CMa

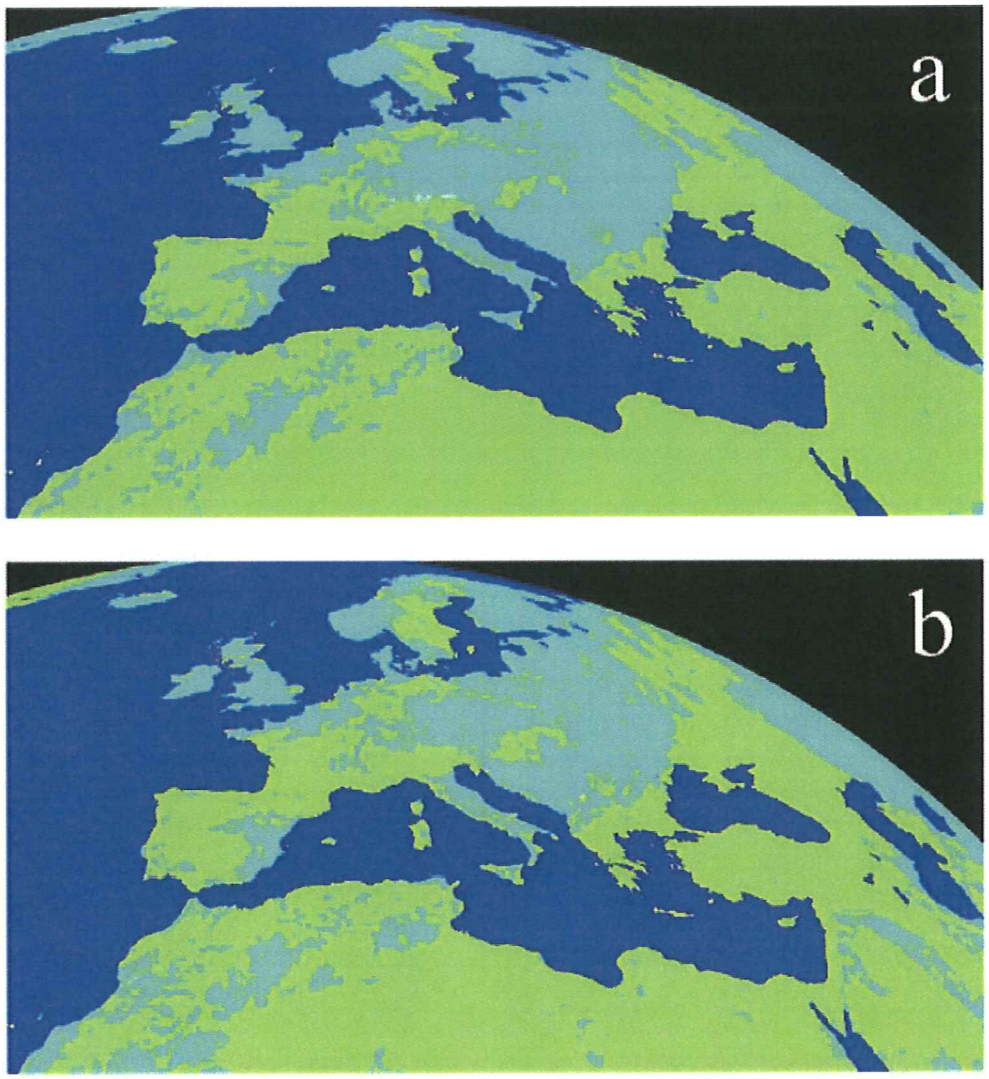

Figure 4.2: snow in white, cloud in cyan, land in green, water in blue a) The tested cloud cover product b) CMa product of SAFNWC on 19^{th} September 2007

and CT products have significantly improved the tested cloud masking product. After several tests done with CMa and CT products, it has been observed that adding 3 classes of CT product (pixel value 12: high opaque and stratiform clouds, pixel value 14: very high opaque and stratiform clouds, and pixel value 17: high semitransparent thick clouds) to the full cloud pixels of CMa product has mostly represented the real cloud cover.

Most thresholds used by these two algorithms were computed from ancillary data such as atlas, climatology maps and numerical weather prediction (NWP) model forecast fields using RTMs for solar bands and Radiative Transfer for TIROS Operational Vertical Sounder (RT-TOVS) for thermal bands (Derrien and Le Gleau, 2005).

SAFNWC generates online cloud cover maps and uses more spectral channels in cloud detection than for the tested cloud masking product, and RTM making CMa and CT products more reliable, a combination of SAFNWC CMa and CT products has been used for cloud masking as a part of the proposed snow detection technique. It can be considered as the first activity where two SAFs products are integrated in the product generation chain. More information about the cloud detection algorithm development can be found in Sürer et al. (2008a).

4.2 Snow Recognition Algorithm

Snow cover maps using SEVIRI data have been produced for each 15 minutes cycle between 8:00-15:45 GMT that makes 32 individual images in a day. All individual 15 minute images acquired during a day are subjected to a series of thresholding tests. First, the high visible reflectance of snow was considered and pixels having reflectance values higher than 0.3 μm are collected. Then, one of the spectral indices similar to the one (Dozier, 1989) has used, called snow index (SI) has been used by dividing NIR 1.6 to VIS 0.6. The pixels having NIR 1.6 / VIS 0.6 values lower than a fixed threshold value 0.8 have been collected. Then, pixels having low sun zenith angle (sza) are discarded by a filter accepting pixels only higher than 5 °. A final test for covering all cold pixels below freezing point has been applied and pixels having temperature lower than 275 K ° on Channel 9 (IR 10.8) are accepted considering that the temperature of snow can not exceed the freezing point (Romanov et al., 2003). After finding snow cover maps for each individual 15 minutes, a daily snow cover map has been generated by accepting pixels having at least 3 snow hits among 32 images during a day. Finally, a daily thematic map has been generated which is consisting of 3 classes: snow, cloud and land as depicted in Figure 4.3.

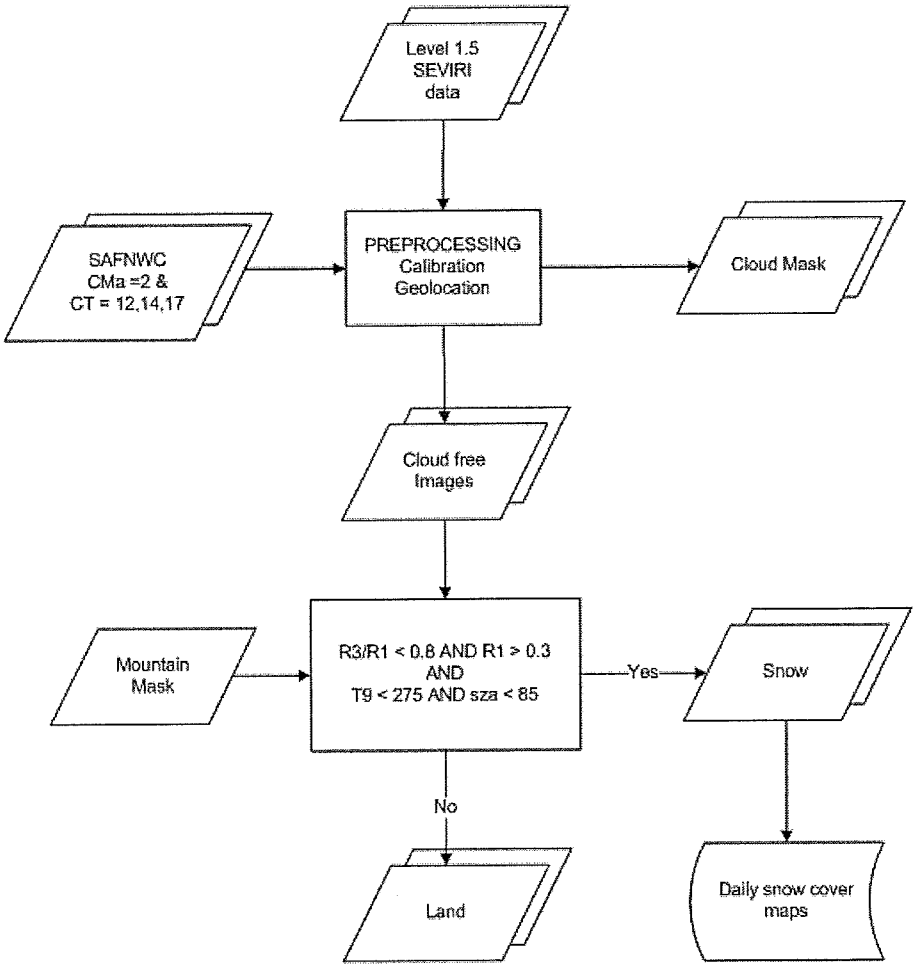

Figure 4.3: Flowchart of the snow cover mapping algorithm

CHAPTER 5

DISCUSSION OF THE RESULTS

Daily snow cover maps of given domain have been produced by the developed algorithm since September 2006. The algorithm is operational on a dedicated server at Turkish State meteorological Services (TSMS) and producing near-real time daily snow cover maps. Several analysis have been made in order to test the performance and accuracy of the developed SR algorithm. The following sub-sections are giving details about the validation analysis of the generated SR products.

5.1 Relationship Between Land Cover Types and Snow Pixels

In this section a visual comparison of developed SEVIRI SR product and MODIS snow cover product, and the relationship between the pixels determined as snow by SEVIRI SR product and land cover types has been investigated. In order to analyze the performance of the algorithm on different weather conditions, date 13^{th} January 2008 has been selected which was a partly cloudy day when there was significant amount of snow on the ground. The image shown in Figure 5.1 b is the final snow cover map product of the developed algorithm, where a red pixel represents snow, cyan represents cloud and green represents land. In order to see the agreement with the real image an RGB composite of the SEVIRI image belonging to the same date at 09:30 scanning time was prepared as shown in Figure 5.1, which was made from the combination of 4 channels in a way that reflects the spectral characteristics of

snow best: VIS 0.6 as red, NIR 1.6 as green and (IR 3.9 - IR 10.8) as blue. As a result of this combination, snow pixels appeared as red since snow has the highest visual reflectance values on VIS 0.6 band interval and low reflectance on NIR 1.6 and (IR 3.9 - IR 10.8) band intervals. Green pixels represent land cover without snow and no cloud interference above. It is observed from the comparison of Figure 5.1 a and Figure 5.1 b that the algorithm has the ability to detect snow covered pixels even stays below clouds during most of the day owing to low repeating cycle time of images.

The landuse map, originally having 6 forest classes, has been divided into 3 main classes as evergreen forest, deciduous forest, and mixed forest in order to observe the distribution of main forest types over the mountainous regions that snow cover has been detected (Figure 5.1 c). In the a and b sections of Figure 5.2 and Figure 5.3, two main mountainous parts of our imaging domain has been compared with MODIS snow cover products. In the Figure 5.2 a, because of its low temporal resolution, MODIS can not determine the snow pixels located on Pyrenees that are covered by clouds at that instant of time. As shown in Figure 5.2 b, for the same location SEVIRI SR algorithm is able to detect even most of the peculiarities of snow cover.

Through overlay analysis covering several mountains of Europe, it has been observed that the snow pixels overlaying with forests are distributed in a percentage such as: 38 % evergreen forest, 46 % deciduous forest, and 16 % mixed forest. The closer view on mountains of Turkey (Figure 5.3), there are minor differences of snow cover extent in the middle coast of Black Sea Region indicated with area of interest (AOI) in Figure 5.3. MODIS snow cover product (Figure 5.3 a) detects patches of snow at this area but SEVIRI SR product (Figure 5.3 b) shows clear land for the same area. This particular subset of image has the landuse distribution percentage as: 64 % evergreen, 24 % deciduous, and 12 % other land. Thus, regarding to the land use studies, it comes out that the algorithm mainly has difficulties in detecting snow for the land cover of deciduous forest type.

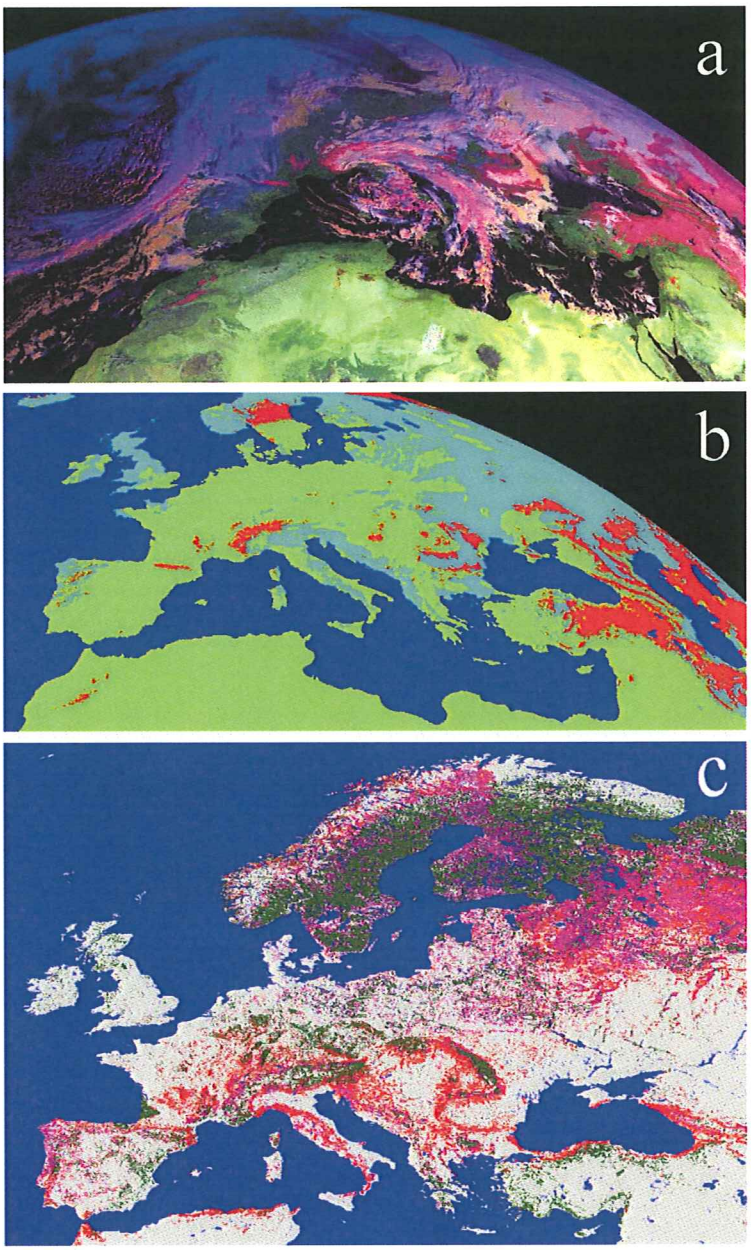

Figure 5.1: a) RGB composite of SEVIRI VIS 0.6 (red), NIR 1.6 (green), IR 3.9-IR 10.8 (blue), starting scan time 09:30 b) Daily SR product of METU for 13^{th} January 2008 snow (red), cloud (cyan), land (green), water (blue) c) Landuse map of Europe, evergreen forest (brown), deciduous forest (red), mixed forest (magenta), other land (gray).

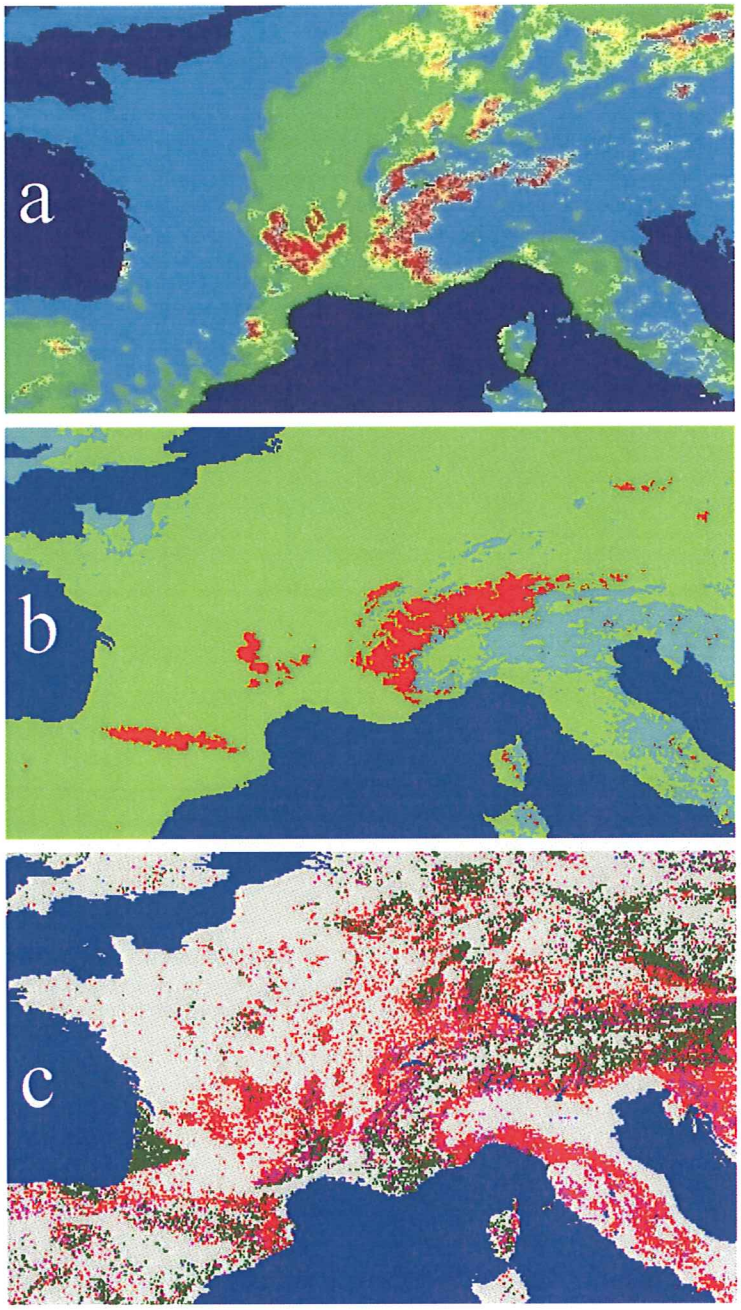

Figure 5.2: a) Daily SR product of MODIS over Alps for 13^{th} January 2008, snow (red), partial snow (yellow), cloud (cyan), land (green) b) Daily SR product of METU over Alps for 13^{th} January 2008, snow (red), cloud (cyan), land(green), water (blue) c) Landuse map of area, evergreen forest (brown), deciduous forest (red), mixed forest (magenta), other land (gray).

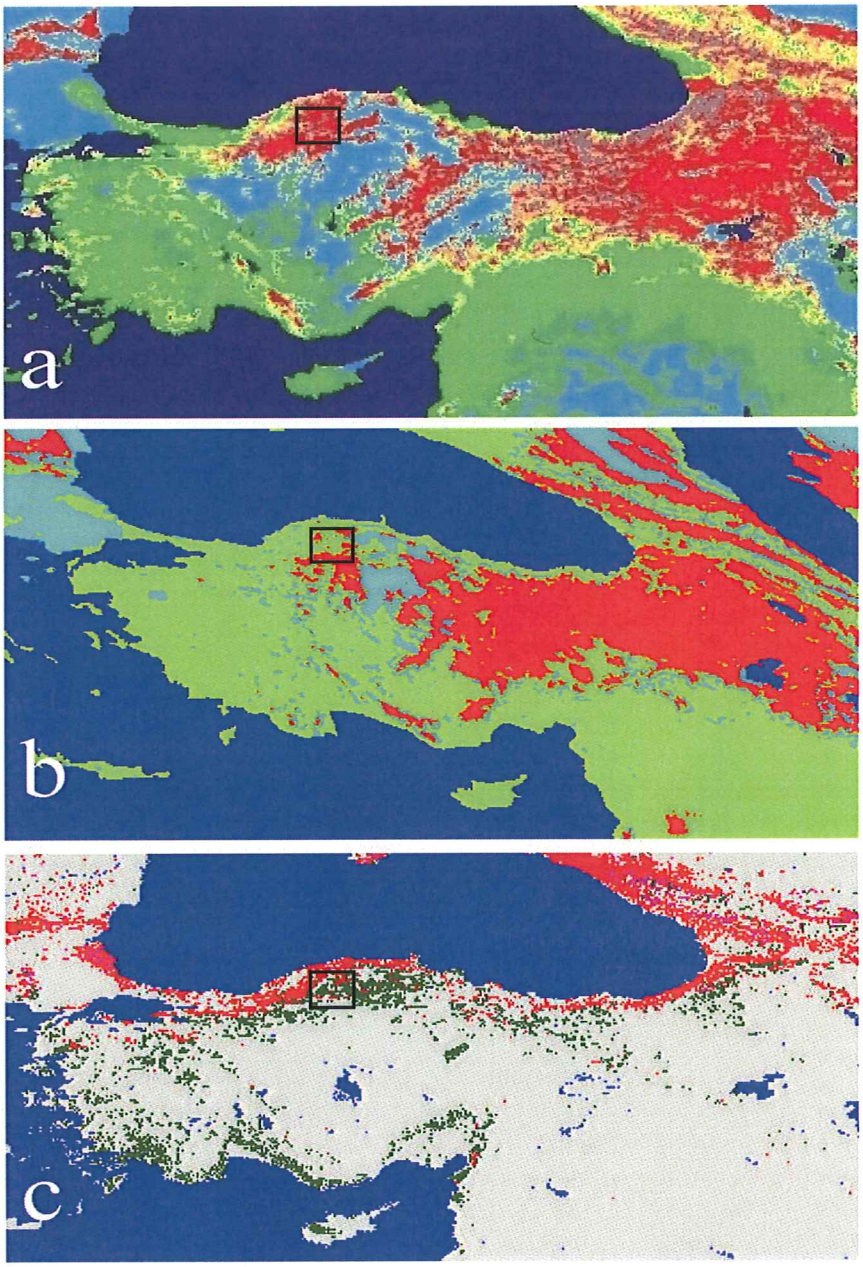

Figure 5.3: a) Daily SR product of MODIS over Turkey for 13^{th} January 2008, snow (red), partial snow (yellow), cloud (cyan), land (green) b) Daily SR product of METU over Turkey for 13^{th} January 2008, snow (red), cloud (cyan), land(green), water (blue) c) Landuse map of area, evergreen forest (brown), deciduous forest (red), mixed forest (magenta), other land (gray).

In the classification results shown in Figure 5.2 and Figure 5.3, the spatial distribution of the snow cover agrees well with the corresponding MODIS snow cover products. There is a slight underestimation of snow cover extent on the resultant snow cover maps which might be a result of narrow threshold intervals or the low solar elevation conditions. Snow cover mapping results of the developed algorithm will most probably show a better performance in the late winter time or in the fall when longer day times and higher sun elevation conditions occur.

5.2 Comparison of SEVIRI and AVHRR/3 Snow Recognition Products

For further testing of the developed SR product's performance, a daily comparison of the SEVIRI SR product with the SR product generated from single NOAA AVHRR/3 data belonging to 19^{th} January 2008 has been performed. This particular day has been selected in order to comply with HydroSAF procedures instead of 13^{th} January 2008. First, an overlay analysis of two products is discussed in Section 5.2.1 , then the correlation of two SR products with elevation has been investigated in Section 5.2.2, and finally the validation of the two SR products with ground observations has been presented in Section 5.2.3. A representative RGB image (Figure 5.4) having the same band combination with Figure 5.1 a is also given for better visual interpretation.

Using this popular RGB combination in snow mapping, the difference between main classes also became more apparent. Water clouds appear as white due to showing high values on all of the three color combinations. Some cold clouds appear as purple and even red, showing similar spectral characteristics with snow and making the discrimination between cloud and snow pixels difficult. At this particular time of 19^{th} January 2008, it is possible to test the SR algorithm especially on cloud clear parts of the image such as the snow covered areas of Eastern Turkey.

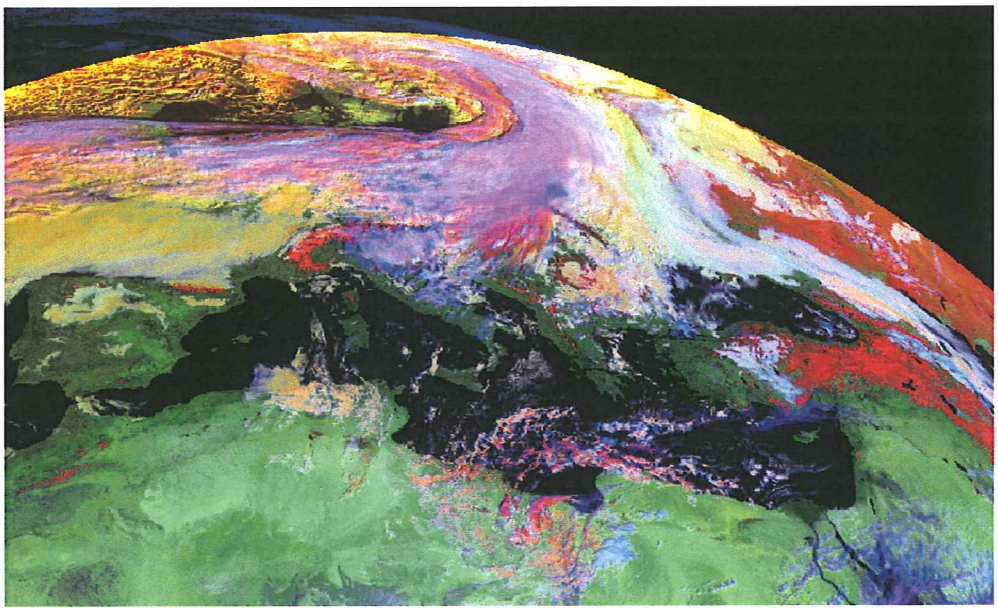

Figure 5.4: RGB composite for 19^{th} January 2008

5.2.1 Overlay Analysis of Snow Recognition Products Obtained from SEVIRI and AVHRR/3

An overlay analysis has been applied to SR products generated from both SEVIRI and AVHRR/3 sensors in order to have better comprehension about the snow recognition abilities of two sensors, as displayed in Figure 5.5. The same SR algorithm was applied for both of the images and also their cloud coverages were obtained from the same SAFNWC CMa and CT products. It should be remembered that the SR product generated from SEVIRI sensor uses 32 sequential images from 08:00 - 15:45; on the other hand the SR product of AVHRR/3 uses only 2 adjacent images mosaicked to cover the same domain as SEVIRI provides. In order to perfectly match the pixels of two SR products used in overlay analysis, the SEVIRI SR product has been reprojected to the projection system of AVHRR/3, Geographic (Lat/Long) projection system having same datum and spheroid as World Geodetic System 1984 (WGS84). Moreover, AVHRR/3 SR product has been resampled from 1.1 km to 5 km spatial resolution, same as SEVIRI SR product. In Figure 5.5, while red color is showing the snow pixels that were detected only by SEVIRI, the

color magenta is representing the snow pixels detected only by AVHRR/3 sensor, and the white color was assigned to the snow pixels that were detected by both of the sensors. From the number of pixels information for each class on this classified image, it has been observed that the 50 % of the areal coverage of the total snow cover was detected only by SEVIRI sensor, 10 % of the snow cover was detected only by AVHRR/3 sensor, and the resting 40 % of the total snow cover was detected by both of the sensors. The low temporal resolution of the AVHRR/3 sensor causes it to detect less number of snow pixels than SEVIRI detects.

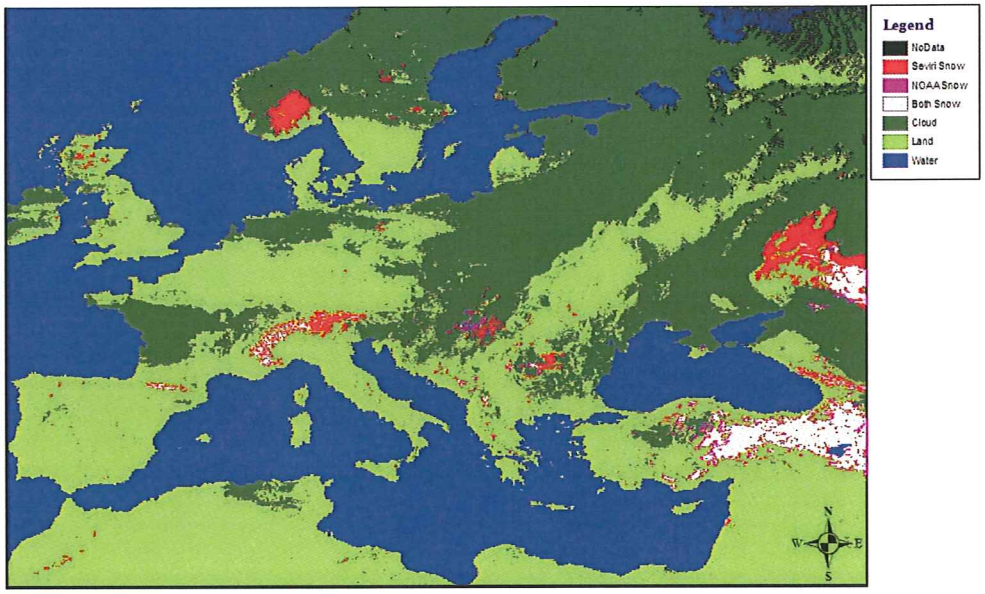

Figure 5.5: Overlay of SR products of SEVIRI and AVHRR/3 for 19^{th} January 2008

As can be seen in Figure 5.5, red pixels (snow detected only by SEVIRI) are mostly located at upper part and left-hand side of the image, this is mainly due to AVHRR/3 having lack of adequate reflectance values information because of high viewing zenith angles at that instant of time. In addition, it was observed that SEVIRI also detects more or less the same amount of snow pixels while using only one image other than 32 composite images for that particular time of the day.

Moreover, because AVHRR/3 has very low temporal frequency of measurement, it is difficult to detect snow pixels lying under moving clouds with SR product obtained from AVHRR/3 data, it is more obvious when comparing Figure 5.4 and Figure 5.5, the Eastern part of the Alps is covered with clouds (in Figure 5.4) and the same area is assigned with red pixels (in Figure 5.5) which are the snow pixels detected only by SEVIRI.

Thus, SEVIRI is able to detect 90 % of the total snow cover, this is mostly because of its high temporal frequency. So, it can also detect snow pixels lying under moving clouds for some part of the day. It was also observed that the SR product derived from AVHRR/3 data has the ability to detect snow pixels present on the lower elevations near snow line boundary (snow/no-snow), because of its better spatial resolution than SEVIRI. The most important contribution to the success of SR algorithm is surely having observations from a geostationary satellite sensor, MSG-SEVIRI which provides a high temporal frequency measurement with spectral information required for accurate snow mapping.

5.2.2 The Correlation of Snow Recognition Products with Elevation

An additional analyze with the SR products of two sensors for 19^{th} January 2008, in order to interpret the relation of snow detection capabilities of SEVIRI and AVHRR/3 with elevation has been done using GTOPO DEM. It was observed that while the mean elevation of the red pixels (snow detected only by SEVIRI) was around 1300 m, the mean elevation of magenta (snow detected only by AVHRR/3) pixels was below 1200 m, indicating that AVHRR/3 has better ability to catch snow pixels on lower elevations. On a region of interest covering only the Eastern Turkey, it was also observed that the snow pixels detected only by SEVIRI were nearly 300 m higher mean elevation than the snow pixels detected only by AVHRR/3. It can easily be seen from Figure 5.5 that the magenta pixels on Eastern Turkey are mostly located around the mountains which are located at lower elevation zones. The reason why AVHRR/3 SR product detects more snow pixels than SEVIRI SR

product on lower elevations (possible fractional snow) is most probably due to its better spatial resolution than SEVIRI.

5.2.3 The validation of Snow Recognition Products with Measurements of Synoptic Weather Stations

Besides comparison of SEVIRI SR product with another SR product obtained from a sensor which has better spatial resolution, the validation of SR products (SEVIRI and AVHRR/3) has been done with 54 synoptic stations distributed over Europe (Figure 5.6, Figure 5.7).

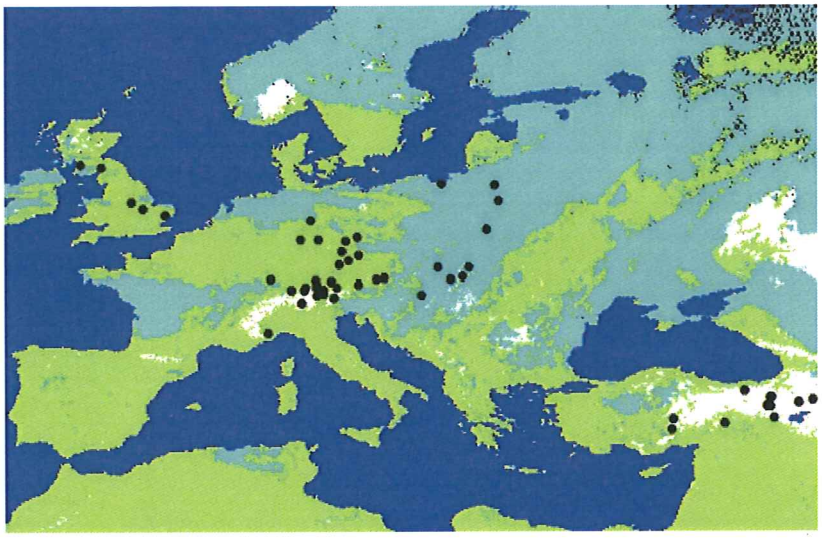

Figure 5.6: Black dots representing the distribution of 54 synoptic weather stations used for validation of MSG-SEVIRI SR product of 19^{th}January 2008 on thematic snow cover map (snow in white, cloud in cyan, land in green, water in blue)

Out of available 54 synoptic stations that have measured snow depth on 19^{th} January 2008, 43 of them were used since 11 stations were falling over the cloud covered regions on 19^{th} January 2008. The 1.1 km spatial resolution AVHRR/3 SR product was resampled to 5 km which is the spatial resolution of SEVIRI SR product in order to have an agreement between pixels of two thematic SR maps due

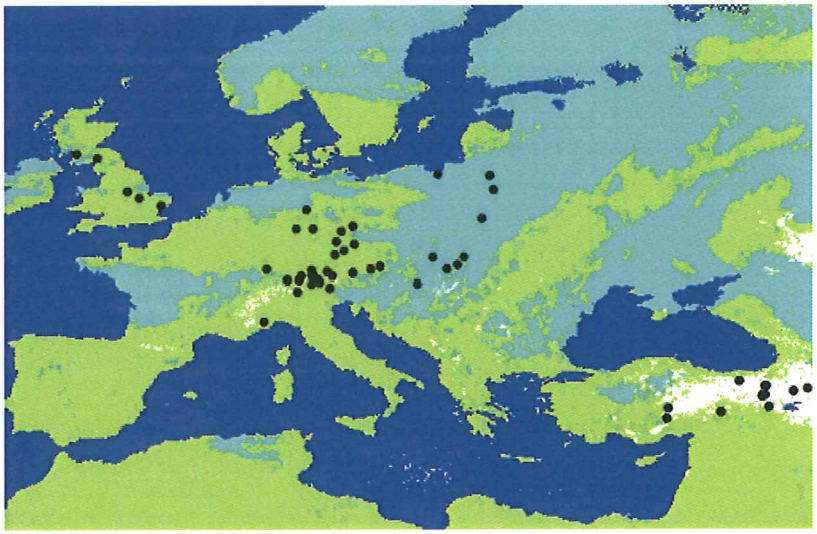

Figure 5.7: Black dots representing the distribution of 54 synoptic weather stations used for validation of NOAA AVHRR/3 SR product of 19^{th}January 2008 on thematic snow cover map (snow in white, cloud in cyan, land in green, water in blue)

to the limitations of the SR product from HydroSAF point of view. The snow data measured by synoptic weather stations are on a point scale. On the other hand, resulting SR maps would have 25 km^2 (5x5) areas for one single pixel.

Table 5.1: Accuracy assessment test results of SEVIRI SR product with synoptic stations

	Synoptic Measurements				
SEVIRI SR product	Snow	Land	Total	Users Accuracy	Producers Accuracy
Snow	20	0	20	100 %	62.5 %
Land	12	11	23	52.1 %	0 %
Total	32	11	43	Overall Avg.	= 74.4 %

Having these facts in mind, the two classes of SR products: snow and land, are

Table 5.2: Accuracy assessment test results of AVHRR/3 SR product with synoptic stations

	Synoptic Measurements				
AVHRR/3 SR product	Snow	Land	Total	Users Accuracy	Producers Accuracy
Snow	14	0	14	100 %	43.75 %
Land	18	11	29	38 %	0 %
Total	32	11	43	Overall Avg.	= 58.1%

processed for an accuracy test with snow depth measurements of synoptic stations. According to the accuracy test with synoptic stations, 74.4 % overall accuracy for SEVIRI SR product (Table 5.1), and 58.1 % overall accuracy for AVHRR SR (Table 5.2) product has been determined. Further discussions about the comparison of these two SR products can be found in a preceding study (Sürer et al., 2008b).

5.3 Validation of SEVIRI Snow Recognition Product Over Turkey with Ground Observations

The performance of the snow recognition (SR) algorithm was further tested with measurements from a densely distributed ground observations network consisting of 78 weather stations (Figure 5.8) over eastern and mountainous parts of Turkey. Observations were covering 17 days in January, 10 days in February, and 10 days in March of 2008.

For validation of the SR products, first three months of the year 2008 have been selected in order to be able to observe the maximum amount of snow in late January and in February, and to detect the melting period in March. 1015 point snow depth observation were used for validation where 395 of them were observed in January, 214 in February, and 406 in March of 2008.

Validation stage of the SEVIRI SR product for the selected days from the first

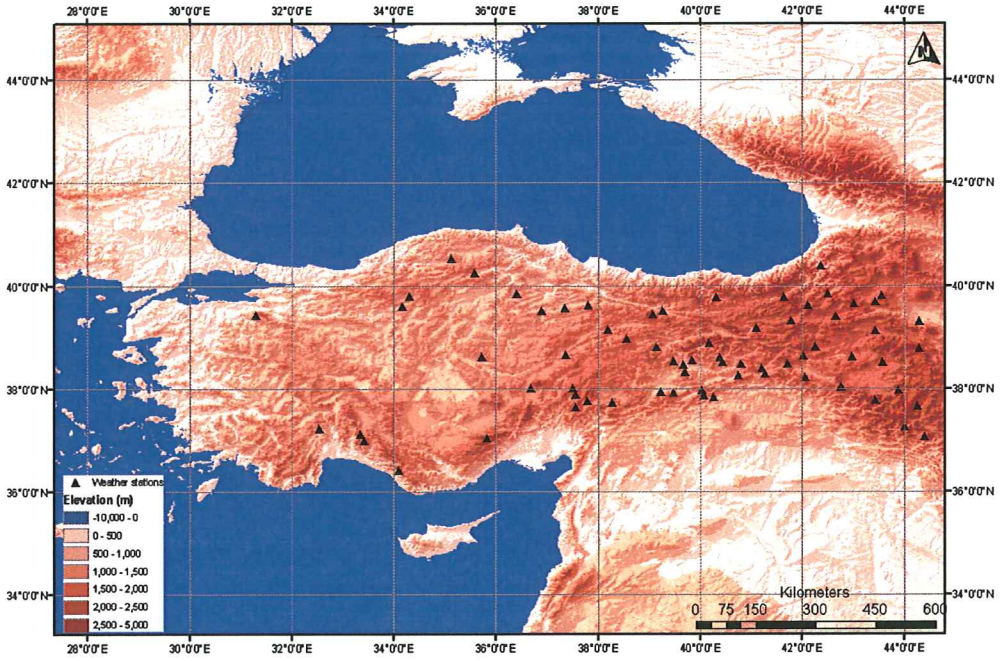

Figure 5.8: The distribution of weather observation stations over DEM of Turkey

3 months of the year 2008 with ground measurements consists of calculation of number of the contingency elements for each of the months and discussion of the resulting outcome. Four commonly used verification metrics in comparison have been calculated as listed in Table 5.4 from the number of contingency elements in Table 5.3 as explained in Section 3.3.

Calculated Bias scores indicate whether the SEVIRI SR product has a tendency to underestimate (Bias lower than 1) or overestimate (Bias greater than 1) events. According to the Table 5.4 the closest score of Bias to 1 which means perfect result, is obtained in month of February, 2008. On the other hand, there is a slight underestimation of snow detection capability of the SEVIRI SR product for March, 2008. On overall, 0.91 Bias score of the SEVIRI SR product has been calculated for three months period.

Probability of detection (POD) score for each month has been calculated very close to 1, perfect result. The SEVIRI SR product has shown great success of detecting

Table 5.3: Summary of contingency element scores calculated for the validation of SR product during first 3 months of 2008.

Contingency elements	January 2008	February 2008	March 2008	Total
a	326	193	316	835
b	0	2	8	10
c	33	6	55	94
d	36	13	27	76
Total	395	214	406	1015

Table 5.4: Calculated metrics for the validation of SR product during first 3 months of 2008.

Metrics	January 2008	February 2008	March 2008	Total
Number of days	17	10	10	37
Bias	0.91	0.98	0.87	0.91
POD	1	0.99	0.98	0.99
FAR	0.09	0.03	0.15	0.10
TS	0.91	0.96	0.83	0.89

snow pixels for all three months period of 2008 according to the POD scores. Since, POD is very sensitive to hits ignoring false alarms, it should be considered together with the FAR scores in order not to cause any misconception.

False alarm ratio (FAR) shows sensitivity to the false alarms, but ignores misses. FAR answers the question of "What is the fraction of the predicted 'yes' events actually did not occur?". According to the calculated FAR scores (Table 5.4), in the month February, 2008 SEVIRI SR product detects very small amount of false snow pixels giving 0.03 FAR score where 0 is the perfect result. In March 2008, the SEVIRI SR product detects 15 % false snow pixels showing correlation with the relatively lower Bias score 0.87. Considering the 0.09 and 0.15 FAR scores for January and March 2008 respectively, the POD scores of these two months (1 and 0.98) might be considered not so realistic and expected to be lower. FAR for three

months period has been calculated as 0.10 meaning only 10 % of total snow pixel detection were false alarms.

Threat score (TS) also known as critical success index (CSI) is sensitive to hits but penalizes both misses and false alarms. TS can be accepted of as the 'accuracy' when correct negatives have been removed from consideration. In March 2008 SEVIRI SR product, giving TS score of 0.83, shows the worst ability to detect snow pixels when compared to other two months. Again in February 2008, the TS has been calculated 0.96 as very close to 1, the SEVIRI SR product gives the best results.

After analyzing each metric scores calculated for the first three months of 2008, it is possible to say that POD scores do not reflect completely the real performance of SR algorithm. Bias and TS seems to represent the algorithm characteristics best. Thus, according to the validation results of SEVIRI SR product for three months period with ground observations over Eastern-Turkey, the SR algorithm has an accuracy of 90 % on snow recognition.

CHAPTER 6

CONCLUSIONS AND RECOMMENDATIONS

6.1 Conclusions

Snow is one of the main water resources, therefore monitoring and estimating the snow covered area play an important role in predicting the amount of snow for winter seasons. The difficulty in accessibility to perform the measurements at the remote sites makes the use of satellite images and/or aerial photographs in monitoring and estimating the snow parameters more valuable.

In the framework of HydroSAF Project, financially supported by EUMETSAT, Turkey is responsible for both the development and calibration/validation of satellite-derived snow products (snow recognition (SR), effective snow cover and snow water equivalent). In this study the development and validation of SR product has been discussed.

In order to obtain SR product over mountainous areas of Europe from optical satellite imagery, spectral thresholding methods were applied on sub pixel scale. Using different spectral characteristics of cloud, snow and land on the electromagnetic spectrum was the main idea while developing algorithm structure. The snow cover mapping methods have generally been used as combinations of satellite observations in the visible, near-infrared, shortwave-infrared and infrared parts of the electromagnetic spectrum. Observations in the visible, near-infrared, and

infrared channels have formed the algorithm aiming the generation of SEVIRI SR product presented in this study.

The satellite images acquired every 15 minutes from geostationary satellite MSG-SEVIRI (Meteosat-9) have been used for the SR algorithm development. Also, the cloud products of SAFNWC have been integrated into the SEVIRI SR algorithm as the cloud detection part. All of the satellite data and terrestrial measurements were stored on a server computer at Turkish State Meteorological Services (TSMS) dedicated for the use of SEVIRI SR product development studies.

Discrimination of cloud and snow pixels have always been the most challenging task at snow cover mapping studies. After developing a specific cloud detection algorithm and verifying it with the cloud mask (CMa) product of SAFNWC, a combination of CMa and cloud type (CT) has been integrated into the SEVIRI SR algorithm as the cloud detection part. Removal of cloud pixels made possible to distinguish snow from land in the developed algorithm. Thresholding of reflectance and temperature values obtained from spectral channels of SEVIRI on a pixel scale has been applied for SR algorithm development including snow index (SI) which is a commonly used index for snow cover mapping.

Covering the domain of HydroSAF Project, daily snow cover maps have been produced by the developed algorithm since September 2006. The accuracy and performance of the generated SR products have been tested by three main analysis. Firstly, a visual interpretation and comparison of SEVIRI SR product with MODIS snow cover product has been applied. The early results were quite encouraging. Investigation of relationship between the pixels determined as snow by SEVIRI SR product and land cover types has shown that the algorithm mainly has difficulties in detecting snow falling over the land cover of deciduous forest type. Secondly, a daily comparison of the SEVIRI SR product with the SR product generated from single NOAA AVHRR/3 data belonging to 19^{th} January 2008 has been performed. It has been observed by the overlay analysis that SEVIRI SR product is able to detect 90 % of the total snow cover by the advantage of its high temporal resolution. Although SEVIRI detected more snow pixels than AVHRR/3 on overall, AVHRR/3

was able to detect more pixels than SEVIRI on lower elevations by courtesy of its higher spatial resolution than SEVIRI. Moreover, a 74.4 % accuracy for SEVIRI SR product with the ground measurements from synoptic stations have been calculated while it was 58.1 % for AVHRR/3. Finally, the performance of the SR algorithm was validated with measurements from ground observations network consisting of 78 weather stations over Turkey. After analyzing several metric scores calculated for the selected days from first three months of 2008, it has been observed that SEVIRI SR algorithm has an accuracy of 90 % on detection of snow pixels.

As a result, the developed SR algorithm for snow cover mapping over mountainous terrain of Europe has shown good performance according to accuracy tests and validation studies. The real time generation of the SEVIRI SR product will continue in the following periods.

6.2 Recommendations

The generated snow cover maps with the developed algorithm will be available to the end users through EUMETCAST. The scientists in the universities and organizations involved in climatology, hydrology and the other earth sciences would use the products in their studies. In Turkey State Hydraulic Works and Turkish State Meteorological Services are the primal potential end-users of the real-time generated SR products.

For the climatological applications in order to get rid of the cloud cover problem, the successive products can be processed and cloud gaps can be filled. Producing a cloud gap filled snow product can be a further study.

Instead of dividing snow cover into two classes as snow on mountain and non-mountain areas, a different classification system suggested by Sturm et al. (1995) that classifies snow into 6 classes (tundra, taiga, alpine, maritime, prairie, and ephemeral) where each class defined by a unique ensemble of textural and stratigraphic characteristics including the sequence of snow layers, their thickness, density, and the crystal morphology and grain characteristics within each layer can be inves-

tigated for further studies.

The accuracy of the snow cover mapping studies mostly depend on the developed algorithm's performance of truly detecting clouds. On very cloudy days it is not possible to make accurate snow cover mapping with using only optical satellite sensors. Since the microwave (MW) satellite observations can penetrate through clouds, it is possible to use blended version of optical and MW observations in order to solve the cloud obstruction problem on very cloudy days. Regarding to this issue, scientists of HydroSAF project are taking place in a study at NASA Goddard Space Flight Center for the development of a blended snow-cover product ANSA which utilizes the Moderate-Resolution Imaging Spectroradiometer (MODIS) standard daily global (5 km resolution) snow-cover product (Hall and Riggs, 2007) and the Advanced Microwave Scanning Radiometer for EOS (AMSR-E) standard daily global (25 km resolution) snow-water equivalent (SWE) product (Kelly et al., 2003) to map snow cover and SWE. It is expected that ANSA product will significantly improve the snow cover mapping performance especially on cloudy days.

REFERENCES

Ackerman, S. A., Strabala, K., Menzel, P., Frey, R., Moeller, C., and Gumley, L. 1998. Discriminating clear sky from clouds with modis. *Journal of Geophysical Research*, 103:32141–32157.

Ackermann, J. 2004. Eps ground segment - avhrr l1 product generation specification. Technical report, EUMETSAT.

Arking, A. and Childs, J. D. 1984. Retreival of cloud cover parameters from multispectral satellite images. *Journal of Climate and Applied Meteorology*, 24:322–333.

Baum, B. and Trepte, Q. 1999. A grouped threshold approach for scene identification in avhrr imagery. *Journal of Atmospheric and Oceanic Technology*, 16:793–800.

Baumgartner, M. F. and Rango, A. 1995. A microcomputer-based alpine snow-cover analysis system (ascas). *Photogrammetric Engineering and Remote Sensing*, 61(12):14751486.

Calle, A., Casanova, J. L., and Romo, A. 2006. Fire detection and monitoring using msg-seviri data. *Journal of Geophysical Research*, 111:G04S06.

Cermak, J. and Bendix, J. 2008. A novel approach to fog/low stratus detection using meteosat-8 data. *Atmospheric Research*, 87:279–292.

Cihlar, J., Belward, A., and Govaerts, Y. 1999. Meteosat second generation opportunities for land surface research and applications. Technical report, EUMETSAT.

de Ruyter de Wildt, M. R., Seiz, G., and Gruen, A. 2007. Operational snow mapping using multitemporal meteosat seviri imagery. *Remote Sensing of Environment*, 109:2941.

Derrien, M. and Le Gleau, H. 2005. Msg/seviri cloud mask and type from safnwc. *International Journal of Remote Sensing*, 26:4707–4732.

Dozier, J. 1989. Spectral signature of alpine snow cover from landsat thematic mapper. *Remote Sensing of Environment*, 28:9–22.

Dozier, J. and Marks, D. 1987. Snow mapping and classification from landsat thematic mapper data. *Annals Glaciology*, 9:97–103.

Elder, K., Rosenthal, W., and Davis, R. E. 1998. Estimating the spatial distribution of snow water equivalence in a montane watershed. *Hydrological Processes*, 12:1793–1808.

Ernst, J. A. 1975. Fog and stratus invisible in meteorological satellite infrared (ir) imagery. *Monthly Weather Review*, 103:1024–1026.

EUMETSAT 2005. Msg - meteosat second generation - in orbit-in use.

Eyre, J. 1991. A fast radiative transfer model for satellite soundings systems. Technical report, ECMWF.

Fowler, G. 2006. Msg level 1.5 image data format description. Technical report, EUMETSAT.

Giri Chandra, Zhu Zhiliang, R. B. 2005. A comparative analysis of the global land cover 2000 and modis land cover data sets. *Remote Sensing of Environment*, 94:1:123–132.

Gleick, P. H. 1987. Regional hydrologic consequences of increases in atmospheric co2 and other trace gases. *Climate Change*, 10:137–161.

Govaerts, Y. M., Arriaga, A., and Schmetz, J. 2001. Operational vicarious calibration of the msg/seviri solar channels. *Advanced Space Research*, 28:21–30.

Gupta, R. P., Haritashya, U. K., and Singh, P. 2005. Mapping dry/wet snow cover in the indian himalayas using irs multispectral imagery. *Remote Sensing of Environment*, 97:458469.

Hall, D. and Martinec, J. 1985. *Remote Sensing of Ice and Snow.* Chapman & Hall.

Hall, D. K. and Riggs, G. A. 2007. Accuracy assessment of the modis snow products. *Hydrological Processes*, 21:12:1534–1547.

Hall, D. K., Riggs, G. A., and Salomonson, V. V. 1995. Development of methods for mapping global snow cover using moderate resolution imaging spectroradiometer (modis) data. *Remote Sensing of Environment*, 54:127140.

Hall, D. K., Riggs, G. A. andSalomonson, V. V., and DiGirolamo, N. E. andBayr, K. J. 2002. Modis snow-cover products. *Remote Sensing of Environment*, 83:181–194.

Kelly, R. E., Chang, A. T., Tsang, L., and Foster, J. L. 2003. A prototype amsr-e global snow area and snow depth algorithm. *IEEE Transactions Geoscience and Remote Sensing*, 41(2):230–242.

King, M. D., Platnick, S., Yang, P., Arnold, G. T., Gray, M. A., Riedi, J. C., Ackerman, S. A., and Liou, K.-N. 2007. Remote sensing of liquid water and ice cloud optical thickness and effective radius in the arctic: Application of airborne multispectral mas data. *Journal of Atmospheric and Oceanic Technology*, 21:857–875.

King, M. D., Tsay, S.-C., Platnick, S., Wang, M., and Liou, K.-N. 1997. Cloud retrieval algorithms for modis: Optical thickness, effective particle radius, and thermodynamic phase. Technical report, Nasa Goddard Space Flight Center.

Koskinen, J., Pulliainen, J., Pylkk, P., Lahtinen, P., Takala, M., Oancea, S., Krn, J.-P., Metsmki, S., Eskelainen, M., and Anttila, S. 2007. Operational snow monitoring using satellite observations. In *Geoscience and Remote Sensing Symposium, 2007. IGARSS 2007. IEEE International*, pages 3979–3982.

Kriebel, K.-T. and Amann, V. 1993. Vicarious calibration of the meteosat visible channel. *Journal of Atmospheric and Oceanic Technology*, 10:225–232.

Leroux, C., Deuze, J. L., Goloub, P., Sergent, C., and Fily, M. 1998. Ground measurements of the polarized bidirectional reflectance of snow in the near-infrared spectral domain: comparisons with model results. *Journal of Geophysical Research*, 103(D16):19721 19731.

Nakajima, T., King, M. D., and J., S. 1991. Determination of the optical thickness and effective particle radius of clouds from reflected solar radiation measurements. part ii: Marine stratocumulus observations. *Journal of the Atmospheric Sciences*, 48:728–751.

Nolin, A. and Liang, S. 2000. Progress in bi-directional reflectance modeling and applications for surface particulate media: Snow and soils. *Remote Sensing Reviews*, 14:307 342.

Nolin, A. W. and Dozier, J. 1993. Estimating snow grain size using aviris data. *Remote Sensing of Environment*, 44(2/3):231238.

Painter, T. H., Dozier, J., Roberts, D. A., Davis, R. E., and Green, R. O. 2003. Retrieval of subpixel snow-covered area and grain size from imaging spectrometer data. *Remote Sensing of Environment*, 85:6477.

Painter, T. H., Roberts, D. A., Green, R. O., and Dozier, J. 1998. The effect of grain size on spectral mixture analysis of snow-covered area from aviris data. *Remote Sensing of Environment*, 65:320332.

Qunzhu, Z., Meisheng, C., Xuezhi, F., Fengxian, L., Xianzhang, C., and Wenkun, S. 1983. A study of spectral reflection characteristics for snow, ice and water in the north of china. In *Hydrological Applications of Remote Sensing and Remote Data Transmission (Proceedings of the Hamburg Symposium)*.

Rango, A. 1980. Operational applications of satellite snow cover observations. *Journal of the American Water Resources Association*, 16(6):1066–1073.

Rango, A. and Itten, K. 1976. Satellite potentials in snowcover monitoring and runoff prediction. *Nordic Hydrology*, 7:209–230.

Rango, A. and Martinec, J. 1979. Application of a snowmelt-runoff model using landsat data. *Nordic Hydrology*, 10:225–238.

Reuter, M. 2005. *Identification of cloudy and clear sky areas in MSG SEVIRI images by analyzing spectral and temporal information.* PhD thesis, Free University of Berlin.

Romanov, P. and Tarpley, D. 2006. Monitoring snow cover over europe with meteosat seviri. In *Proceedings of the 2005 EUMETSAT Meteorological Satellite Conference*, pages 282–287.

Romanov, P., Tarpley, D., Gutman, G., and Carroll, T. 2003. Mapping and monitoring of the snow cover fraction over north america. *Journal of Geophysical Research*, 108:8619, doi:10.1029/2002JD003142.

Rosenthal, W. 1996. Estimating alpine snow cover with unsupervised spectral unmixing. In *Geoscience and Remote Sensing Symposium, IGARSS.*, volume 4, pages 2252–2254, Lincoln, NE, USA. IEEE.

Rossow, W. B. and Garder, L. C. 1993. Cloud detection using satellite measurements of infrared and visible radiances for isccp. *Journal of Climate*, 6:2341–2369.

Rott, H. 1984. Synthetic aperture radar capabilities for snow and glacier monitoring. *Advances in Space Research*, 4(11):241246.

Schmetz, J., Pili, P., Tjemkes, S., Just, D., Kerkmann, J., Rota, S., and Ratier, A. 2002. An introduction to msg-seviri. *Bulletin of the American Meteorological Society*, 81:977–1001.

Seidel, K. and Martinec, J. 2004. *Remote Sensing in Snow Hydrology.* Springer.

Shi, J. and Dozier, J. 1997. Mapping seasonal snow with sir-c/x-sar in mountainous areas. *Remote Sensing of Environment*, 59:294–307.

Shiklomanov, I. A. 1990. Global water resources. *Nature and Resources*, 26(3):343–353.

Solberg, R. and Andersen, T. 1994. An automatic system for operational snow-cover monitoring in the norwegian mountain regions. In *Proceedings of IGARSS94 symposium*, page 2084 2086, Pasadena, CA, USA. IEEE.

Sturm, M., Holmgren, J., and Liston, G. E. 1995. A seasonal snow cover classification system for local to global applications. *American Meteorological Society*, 8(5):1261–1283.

Sürer, S., Gökdemir, O., Akyürek, Z., Şorman, A. U., and Beşer, O. 2008a. Snow cover mapping over the mountainous areas of europe with msg-seviri. *EARSeL eProceedings*, - in review.

Sürer, S., Gökdemir, O., Beşer, O., Akyürek, Z., Şorman, A. U., and Ertürk, A. G. 2008b. Real time snow recognition from msg satellite for mountainous areas. In *28th EARSeL Symposium: Remote Sensing for a Changing Europe.*

Tanre, D., Deroo, C., Duhaut, P., Herman, M., Morcrette, J., Perbos, J., and Deschamps, P. 1990. Description of a computer code to simulate the satellite signal in the solar spectrum. *International Journal of Remote Sensing*, 11:659–668.

Tarble, R. D. 1963. Areal distributions of snow as determined from satellite photographs. *International Association of Hydrological Sciences Special Publication*, 65:372–375.

Warren, S. G. 1982. Optical properties of snow. *Reviews of Geophysics and Space Physics*, 20(1):67 89.

Wiscombe, W. J. and Warren, S. G. 1980. A model for the spectral albedo of snow, i, pure snow. *Journal of the Atmospheric Science*, 37(12):2712 2733.

Zhang, N., Wu, Q., and Zhang, L. 2008. Extraction of snow-covered information from remote sensing data of cbers-02 imagery. In *Congress on Image and Signal Processing.*

APPENDIX A

CLIMATE STATIONS

Table A.1: List of 70 big climate stations used for validation (Part-1)

ID	Latitude	Longitude	Elevation (m)
17045	41.18	41.82	628
17084	40.55	34.97	776
17086	40.30	36.57	608
17088	40.47	39.47	1219
17090	39.75	37.02	1285
17094	39.45	39.30	1218
17096	39.95	41.17	1758
17097	40.37	43.06	1775
17099	39.72	43.05	1632
17100	39.92	44.05	858
17160	39.15	34.17	1007
17162	39.18	36.07	1171
17165	39.12	39.55	981
17196	38.43	35.29	1092
17199	38.35	38.22	948
17201	38.39	39.15	989

Table A.2: List of 70 big climate stations used for validation (Part-2)

ID	Latitude	Longitude	Elevation (m)
17203	38.87	40.50	1177
17204	38.68	41.48	1323
17205	38.48	42.30	1665
17285	37.57	43.73	1728
17618	41.35	33.50	1050
17646	40.49	32.54	1126
17650	41.01	34.02	870
17656	40.51	43.2	1688
17664	40.28	32.39	1033
17666	40.48	41.00	1222
17668	40.55	41.98	1322
17676	40.07	29.07	1877
17681	40.18	35.53	717
17682	40.17	38.25	1364
17683	40.24	36.05	529
17684	40.09	38.04	1163
17688	40.30	41.55	1572
17690	40.05	42.17	1540
17692	40.33	42.57	2102
17716	39.54	37.45	1347
17718	39.78	40.38	1425
17720	39.33	44.05	1725
17734	39.37	38.12	1120
17736	39.03	39.60	1400
17740	39.37	41.70	1715
17764	39.05	38.50	1200
17766	38.95	38.72	900
17768	39.07	38.92	953

Table A.3: List of 70 big climate stations used for validation (Part-3)

ID	Latitude	Longitude	Elevation (m)
17774	38.97	40.03	1090
17776	38.97	41.07	1366
17778	39.17	41.45	1650
17780	39.15	42.53	1565
17784	39.02	43.21	1678
17802	38.43	36.24	1500
17804	38.80	38.75	808
17806	38.72	39.97	1000
17808	38.75	40.57	1250
17810	38.46	42.30	1750
17812	38.40	43.59	2100
17840	38.29	36.30	1500
17843	38.34	38.49	1300
17844	38.27	39.19	1240
17846	38.24	39.40	1100
17852	38.18	43.06	1694
17866	38.01	36.29	1344
17868	38.15	36.55	1180
17870	38.12	37.12	1137
17880	38.03	44.01	2400
17882	37.52	30.50	920
17896	37.41	31.44	1148
17898	37.26	31.51	1131
17906	37.32	34.29	1453
17920	37.34	44.17	1877
17928	36.59	32.30	1552